

De Novo Parallel Design, Synthesis and Evaluation of Inhibitors against the Reverse Transcriptase of Human Immunodeficiency Virus Type-1 and Drug-Resistant Variants

Alon Herschhorn,^{‡,§} Lena Lerman,[#] Michal Weitman,[#] Iris Oz Gleenberg,[‡] Abraham Nudelman,^{*,#} and Amnon Hizi^{*,‡,||}

Department of Cell and Developmental Biology, Sackler School of Medicine, Tel Aviv University, Tel Aviv 69978, and Chemistry Department, Bar Ilan University, Ramat Gan 52900, Israel

Received November 12, 2006

We used molecular modeling to design *de novo* broad-range inhibitors against wild type and drug-resistant variants of the reverse transcriptase (RT) of human immunodeficiency virus type-1 (HIV-1). First, we screened for small fragments that would interact with each one of four RT structures (one wild type and three mutants). Then, these fragments were linked to build a scaffold molecule. Out of 27 different compounds that were synthesized, four inhibited the DNA polymerase activity of RT with IC₅₀ values below 10 μM. Compound **5f** inhibited RT with an IC₅₀ value of about 3.5 μM, while inhibiting drug-resistant RT variants more efficiently than the clinically used drug, nevirapine (11-cyclopropyl-5,11-dihydro-4-methyl-6H-dipyrido[3,2-*b*:2',3'-*e*]-[1,4]diazepin-6-one). **5f** also inhibited the RT ribonuclease H activity with an IC₅₀ of 20 μM and therefore, unlike nevirapine, targets both RT activities. Accordingly, **5f** can serve as lead for developing novel inhibitors against RT that may be used to suppress HIV-1 growth.

Introduction

The reverse transcriptase (RT^a) of HIV-1 is an essential enzyme in the retroviral life cycle. After penetrating into the target cell, RT copies the viral plus sense and single-stranded genomic RNA into double-stranded DNA. This process is catalyzed solely by RT and depends on two fundamental enzymatic activities: that of the DNA polymerase (which copies both RNA and DNA into DNA) and that of the RNase H, which concomitantly cleaves the viral RNA strand in the RNA/DNA heteroduplex. The resulting double-stranded DNA is transported into the nucleus as part of a preintegration complex and is subsequently incorporated into the DNA of the cell by the viral enzyme integrase.¹ Since the identification, two decades ago, of HIV-1 as the cause for AIDS, a massive search for molecules that block RT activities has been conducted worldwide. These efforts led to the identification of two classes of anti-RT compounds: nucleoside/nucleotide RT inhibitors (NRTIs) and non-nucleoside RT inhibitors (NNRTIs).² NRTIs are competitive inhibitors that mimic normal nucleotides but lack the 3'-OH. When incorporated into the nascent DNA by RT, NRTIs prevent additional incorporation of nucleotides and, hence, terminate chain elongation. The NNRTIs are a variety of noncompetitive inhibitors that bind specifically to a hydrophobic pocket in

proximity to the DNA polymerase active site of the enzyme;³ most of them are highly specific against HIV-1 RT with minimal effects on the closely related HIV-2 RT.⁴ Both classes of inhibitors are currently used in the therapy against HIV-1 as part of the highly active anti-retroviral therapy, which simultaneously targets the RT, the viral protease, and most recently the entry step of the virus.⁵

A significant obstacle for the use of NNRTIs is their very high specificity that reduces their efficacy against mutated variants of the virus.⁶ Given that the protein targets for therapy, especially the RT and protease, are quite flexible and can tolerate mutations and still remain active, resistance develops rapidly during treatment even when a combination of drugs is used.⁷ Consequently, intense efforts have been directed in recent years to find broad spectrum NNRTIs that inhibit both wild type and drug-resistant variants of RT. This intensive search led to the discovery of several highly efficient inhibitors, including 4-[[6-amino-5-bromo-2-[(4-cyanophenyl)amino]-4-pyrimidinyl]oxy]-3,5-dimethylbenzoxonitrile (TMC-125), *N*-[4-(aminosulfonyl)-2-methylphenyl]-2-[4-chloro-2-(3-chloro-5-cyanobenzoyl)phenoxy]acetamide (GW678248), and 5-bromo-*N*-(4-chloro-5-isopropyl-3-methyl-1,3-thiazol-2(3*H*)-ylidene)-2-hydroxybenzenesulfonamide (YM-215389).^{8–10} However, identifying such inhibitors by screening random libraries and optimizing them by systematic chemical modifications are highly time and resources consuming. Therefore, faster and more efficient strategies that facilitate and shorten the discovery process would be extremely beneficial.

Molecular modeling is one approach that could be used to narrow down a library containing an extraordinarily high number of random molecules into a smaller list of the potentially effective inhibitors. Two major tools that have been used intensively in this arena are virtual screening and *de novo* drug design, both of them based either on the known crystal structure of the specific target enzyme or on known inhibitors against the enzyme. Virtual screening is usually performed by docking each member of a large available chemical database into the enzyme's active site. This leads, in most cases, to a selective list enriched in active compounds. The top scored molecules of such screens can be then easily obtained and tested for

* To whom correspondence should be addressed. A. Hizi, Tel: 972-36409974. Fax: 972-36407432. Email: ahizi@post.tau.ac.il.; A. Nudelman, Tel: 972-35318314. Fax: 972-35351250. Email: nudelman@mail.biu.ac.il.

[‡] Tel Aviv University.

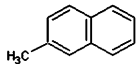
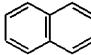
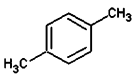
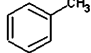
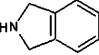

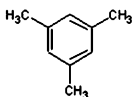
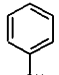
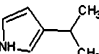
[#] Bar Ilan University.

[§] This work was performed in partial fulfillment of the requirements for a Ph.D. degree of A. Herschhorn, Sackler Faculty of Medicine, Tel Aviv University, Israel.

^{||} The Gregorio and Dora Shapira Chair for the Research of Malignancies.

^a Abbreviations: RT, reverse transcriptase; HIV, human immunodeficiency virus; RNase H, ribonuclease H; AIDS, acquired immunodeficiency syndrome; NRTIs, nucleoside/nucleotide reverse transcriptase inhibitors; NNRTIs, non-nucleoside reverse transcriptase inhibitors; PETT, phenethylthiazolylthiourea; DABO, dihydroalkoxybenzylloxypyrimidine; XTT, 2,3-bis(2-methoxy-4-nitro-5-sulfophenyl)-5-[(phenylamino)carbonyl]-2*H*-tetrazolium hydroxide; NMR, nuclear magnetic resonance; CFF, consistent forcefield; RMS, root mean square; PLP, piecewise linear potential; CI, chemical ionization; DTT, dithiothreitol; EDTA, ethylenediamine tetraacetic acid; TBE, tris borate ethylenediamine tetraacetic acid; dTTP, deoxythymidine triphosphate.

Table 1. Ludi Scores of the Fragments with the Highest Affinity to the NNRTI Binding Pocket of All the Crystal Structures of RT Tested

Fragment	RT crystal structures				
	Wild type	T181C	K103N	L100I + K103N	Average
	598	517	659	665	610
	368	429	651	602	513
	478	327	537	535	469
	459	328	498	514	450
	332	514	507	421	444
	448	366	453	462	432
	378	317	535	388	405
	449	276	321	335	345
	331	324	333	315	326

inhibitory activity against the enzyme.¹¹ The *de novo* design of new molecules is done by first identifying the functional groups that bind the active site of the target protein and then linking them into the final inhibitor molecules. The desired molecules are then synthesized and tested for their enzymatic inhibitory effects.¹²

Since the discovery of NNRTIs, crystal structures of wild type and drug-resistant variants of HIV-1 RT have been used extensively in the design of novel NNRTIs. Mao et al. used a flexible binding site based on several structures to design a few PETT and DABO derivatives with improved profiles against drug resistance mutants of HIV-1 RT.¹³ Moreover, Vinkers et al. have recently designed *de novo* several NNRTIs, using advanced software that includes a synthesis route for each generated molecule.¹⁴

Here, we present a novel approach for *de novo* design of NNRTIs that inhibit wild type as well as drug-resistant variants of HIV-1 RT. We have used four different crystal structures of RT, one wild type and three mutated enzymes, which are resistant to several of the commonly used NNRTIs.^{15,16} On the basis of these structures, we searched for small fragments of synthetic molecules that could bind separately to each variant of the RT enzyme. The fragments that interacted with each RT structure were compared and only those that interacted with all

Table 2. Docking and Scoring of the Scaffold and Control Molecules into the Various RT Structures^a

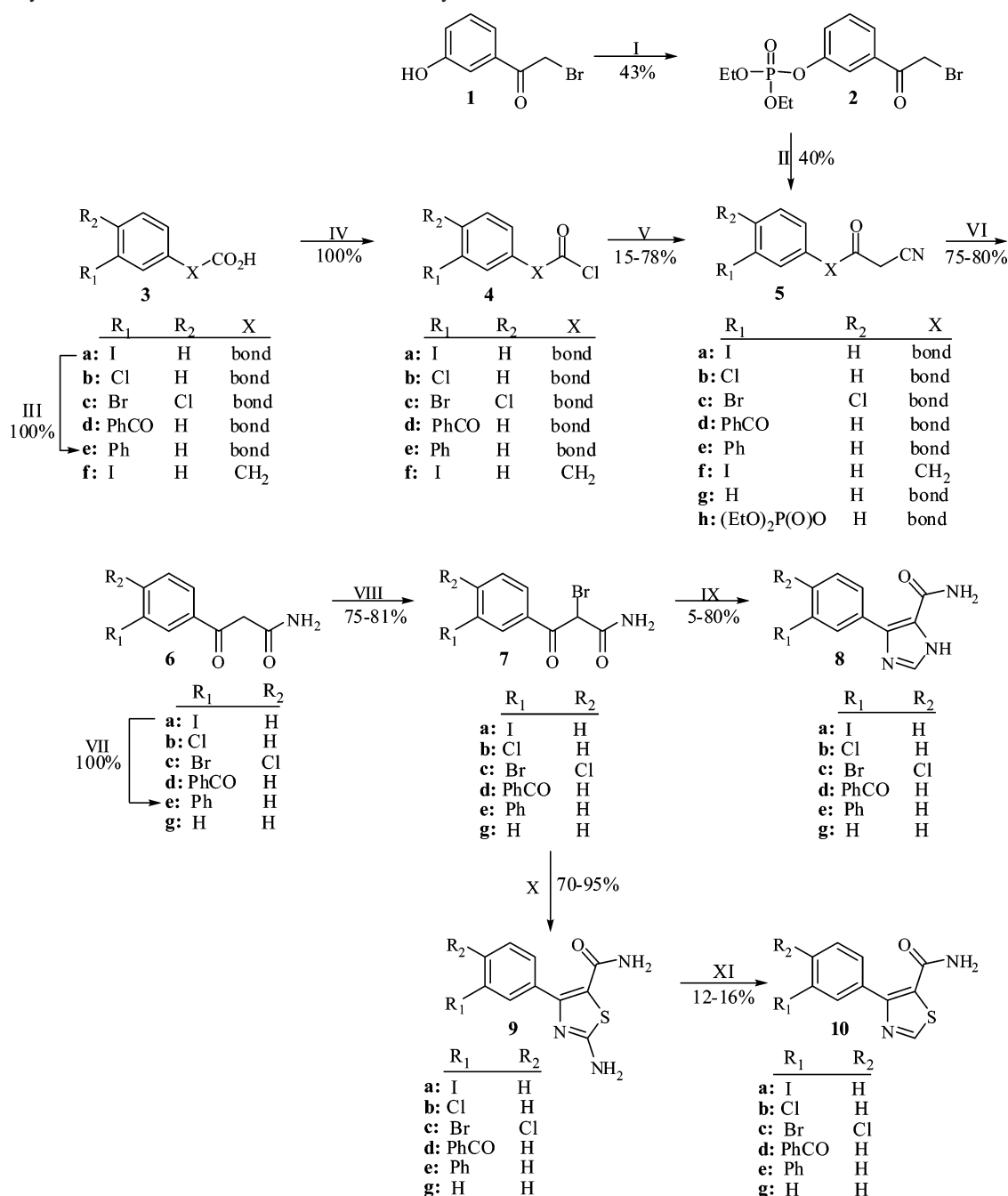
crystal structure	scoring function ^b	efavirenz	scaffold	ref_10087_NCI
		(positive control)	(negative control)	(negative control)
Wild type	Ligscore1	3.56	3.97	2.4
	PLP2	97.31	98.32	64.3
T181C	Ligscore1	3.53	3.85	2.6
	PLP2	101.85	89.93	57.6
K103N	Ligscore1	4.16	4.23	2.7
	PLP2	96.69	97.66	71.8
L100I + K103N	Ligscore1	3.02	4.28	2.5
	PLP2	81.27	97.98	79.1
average	Ligscore1	3.65	4.13	2.56
	PLP2	92.99	94.89	68.19

^a The values reported are the scores of the best conformation for each molecule. ^b The docked molecules were scored using Ligscore1 and PLP2 scoring functions in the ligandfit module of cerius 2. The positive value of PLP2 is reported and in both functions the highest score represent the strongest binding.

four structures were linked together to construct a final compound. The resulting molecule was used as a scaffold for the synthesis of various chemically related molecules that were subsequently tested *in vitro* for inhibiting the activities of HIV-1 RT.

Results

De Novo Design of Non-nucleoside RT Inhibitors. To construct a wide range of NNRTIs against both wild type and drug-resistant HIV-1 RT variants, we used four structures of the RT: wild type, mutant K103N, double mutant K103N + L100I, and mutant T181C. The NNRTI binding site was defined in all four structures, and each one was screened separately against a library of 1000 small fragments using the Ludi module in the Cerius 2 software.¹⁷ Ludi generates a map of interaction sites within the NNRTI binding site based on favorable orientations for H-bonds and hydrophobic contacts.^{18,19} The module then fits different fragments from a library of small molecules (5–30 atoms) onto these sites and scores each fragment according to the bonds that it can make with the RT. Screening against the four RT structures resulted in four separate lists of fragments. In each list, every fragment was scored according to its affinity to the specific NNRTI binding site in the specific structure. The results were filtered to retain only those fragments that appeared in all RT structures, and the scores of these fragments were averaged over all structures. Nine molecules were identified in the search, and their location within the hydrophobic pocket of the NNRTI was verified (Table 1). From this group, the phenyl and pyrrole rings were chosen and were colocalized within the NNRTI binding site in the Ludi module. Using the same module, we conducted a second search to connect the fragments. This search suggested to link the two fragments through a phenyl group and to add an amide group to the pyrrole. In addition, the pyrrole was replaced by an imidazole to simplify the synthesis of such molecules (scaffold, see Table 2).

Scheme 1. Synthesis of the Different Molecules in the Study

To ensure that the novel scaffold molecule can bind the RT in an energetically favorable mode, the molecule was energy minimized and then docked into the NNRTI binding site of all four structures, using the module ligand fit of Cerius 2.²⁰ We performed the same docking with two reference molecules. Efavirenz, a clinically used NNRTI drug, which was originally cocrystallized with RT, was used as a positive control and a random molecule from the NCI database (ref_10087_NCI) was used as negative control (Table 2). The top ranked structures of the docking process were scored with the Ligscore1 and PLP2 scoring functions. These functions showed the best selectivity with negative and positive training sets of molecules against RT in a preliminary analysis (out of the nine scoring functions in ligand fit). The scores from the docking of the scaffold molecule against all structures were averaged and compared to the positive and negative controls (Table 2). As judged from the scoring results, the final molecule exhibited scores compa-

rable to those of efavirenz and fitted the RT structures much better than the negative control molecule, indicating that the new scaffold molecule was a reasonable candidate for further evaluations.

We then synthesized and tested three groups of derivatives of the scaffold molecule. Group I included the phenyl ring attached to an amido substituted imidazole/thiazole (compounds **8a–10f**, Scheme 1). In group II, the amido-substituted heterocyclic ring was replaced with a 2-oxopropanamide fragment (compounds **6a–g**, Scheme 1), and in group III it was replaced with a 2-oxopropanenitrile/2-oxobutanenitrile fragment (compounds **5a–h**, Scheme 1). These replacements were intended to introduce functional groups that were more flexible than those of the scaffold molecule due to the additional rotatable bonds of the molecules. The resulting molecules would presumably have better ability to accommodate themselves in the binding pocket of either the wild type or the mutant RTs. In all three

groups, the phenyl ring was further substituted with either another phenyl group or halogen atoms. In addition, one member of the third group was substituted with a phosphate group.

Chemical Synthesis. Compounds **1**, **3a-d**, **3f**, and **5g** are commercially available and served as primary building blocks for the synthesis. Compound **3e** was prepared by a Suzuki reaction between phenylboronic acid and **3a**.

The synthesis of the various heterocyclic compounds started with the conversion of the carboxylic acids **3a-f** to acyl chlorides **4a-f**. Alkylation of the latter with cyanoacetic acid in the presence of *n*-BuLi gave compounds **5a-f** in about 60% isolated yield. The phosphorylated analogue **5h** was obtained from 2-bromo-3'-hydroxyacetophenone (**1**) in a two-step synthesis involving phosphorylation and replacement of bromide by potassium cyanide. Hydration of the β -ketonitriles **5a-g** in the presence of concentrated H₂SO₄ gave the amides **6a-g**. This step was problematic for compound **5e**, since under these conditions the external electron rich phenyl ring was converted into an arylsulfonic acid.²¹ To overcome this problem, the synthetic sequence was changed, with the introduction of the second phenyl ring following the construction of the amide moiety. On the basis of this strategy, compound **6a** was reacted in a Suzuki reaction with phenylboronic acid to give **6e**. α -Bromination of amides **6a-g** provided **7a-g**, which were used as intermediate building blocks for a variety of heterocyclic rings. The construction of the imidazole moiety suffered from extremely low yields, and numerous attempts were made to improve it. Finally, the imidazoles **8a-g** were synthesized by heating of **7a-g** in formamide to which a few drops of concentrated H₂SO₄ had been added. The aminothiazole derivatives **9a-g** were prepared in good yields by reaction of **7a-g** with thiourea. Deamination of the latter gave the thiazoles **10a-g**.

RT Enzymatic Activity. A total of 27 synthesized molecules were tested against the DNA polymerase activity of HIV-1 RT. The IC₅₀ values, compound concentrations inhibiting 50% of the initial activity of RT, were calculated for each compound from dose-response curves (Table 3). Fourteen compounds inhibited the DNA polymerase activity with apparent IC₅₀ values below 100 μ M, and four showed IC₅₀ values below 10 μ M (Table 3). In group I, out of sixteen molecules, eight displayed IC₅₀ values below 100 μ M. Compounds **10d** and **8c** were the most effective ones in this group with IC₅₀ values of about 16 and 9.9 μ M, respectively. In compound **10d**, the distance between the two phenyl groups was increased by inserting a carbonyl group between them, and in **8c**, Br and Cl atoms were added to the middle phenyl group. In both cases, the inhibitory effect was significantly improved compared to analogous molecules lacking these functional groups (**10e** and **8g**). In group II, only compound **6a** showed a significant inhibitory effect, suggesting a preferred interaction of the iodine in the context of this structure with specific groups in the RT enzyme. In the substances of group III, four out of the six molecules were effective. In compound **5d**, as in **10d**, increasing the distance between the phenyl groups by an insertion of a carbonyl group improved the inhibition relative to molecule **5e**. Addition of a chloride atom in compound **5b** resulted in a potent inhibitor, whereas addition of an iodide atom at the same position (compound **5a**) abolished the activity against RT. Compound **5f**, which possesses a 2-oxobutanitrile substituent is an analogue of **5a**, where the 2-oxopropanitrile found in **5a** is separated from the aromatic ring by an additional methylene group. Interestingly, this extension of the molecule was beneficial and **5f** showed the most effective inhibition with an IC₅₀ value of

Table 3. The Effects of the Different Molecules Synthesized on RT Enzymatic Activities and on the Viability of Jurkat Cells^a

compd	DNA polymerase, ^b IC ₅₀ [μ M]	RNase H, IC ₅₀ [μ M]	CC ₅₀ ^c [μ M]
5a	$\gg 312$	ND	ND
5b	4.1 \pm 0.5	28 \pm 2	$\gg 312$
5c	$\gg 312$	ND	ND
5d	9.8 \pm 2.4	98 \pm 6	251 \pm 18
5e	33.4 \pm 9.6	84 \pm 5	233 \pm 19
5f	3.5 \pm 0.8	20 \pm 1	247 \pm 28
5h	64.3 \pm 16.9	112 \pm 2	$\gg 312$
6a	29.6 \pm 5.7	$\gg 312$	$\gg 312$
6b	$\gg 312$	ND	ND
6d	$\gg 312$	ND	ND
6e	$\gg 312$	ND	ND
8b	79.8 \pm 18.8	$\gg 312$	$\gg 312$
8c	9.9 \pm 1.4	41 \pm 9	213 \pm 3
8d	$\gg 312$	ND	ND
8e	$\gg 312$	ND	ND
8g	300 \pm 84	ND	ND
9a	125.4 \pm 14.2	ND	ND
9b	54.4 \pm 8.9	$\gg 312$	$\gg 312$
9c	118.2 \pm 19.9	ND	ND
9d	44.1 \pm 10.8	$\gg 312$	$\gg 312$
9e	59.2 \pm 7.6	249 \pm 45	244 \pm 8
9g	80.7 \pm 17.6	$\gg 312$	$\gg 312$
10a	$\gg 312$	ND	ND
10c	87.5 \pm 11.2	ND	ND
10d	16.3 \pm 4.6	77 \pm 13	$\gg 312$
10e	$\gg 312$	ND	ND
10g	283.4 \pm 28.6	ND	ND
nevirapine	1.7 \pm 0.2	ND	ND

^a IC₅₀ = concentration of inhibitor at which the specified RT activity was reduced by 50% compared to the inhibitor-free control. ^b DNA polymerase activity was assayed with poly(rA)_noligo(dT)₁₂₋₁₈ substrate, as described under the Experimental Section. ^c CC₅₀ = concentration of inhibitor at which the cell viability was reduced by 50% compared to the inhibitor-free control.

approximately 3.5 μ M. For these studies, nevirapine, a clinically used RT inhibitor was used as reference, its IC₅₀ value under these conditions was 1.7 μ M.

All thirteen compounds with apparent IC₅₀ values below 85 μ M for inhibition of the HIV-1 RT-associated DNA polymerase activity were further tested for inhibition of the RNase H activity of the enzyme. Out of the tested compounds, five did not inhibit this activity even at concentrations as high as 312 μ M, while the other eight molecules showed different degrees of inhibition (Table 3). Compound **6a** inhibited only the DNA polymerase activity and had no effect on the RNase H activity. The inhibition of RT by compound **5d** was more specific to the DNA polymerase activity compared to the inhibition of the RNase H activity, with IC₅₀ values of about 9.8 μ M and 98 μ M, respectively. In contrast, compounds **8c**, **5b**, and **5f** showed broader inhibition and were effective against both activities of RT. Compound **5f** displayed the lowest IC₅₀ value of 20 μ M against the RNase H activity and was the most effective against both activities (Table 3).

Two of the most effective RT inhibitors, compounds **8c** and **5f**, were further evaluated against the DNA polymerase activity of two drug-resistant mutants of HIV-1 RT. T181C, a single mutant RT that carries a cysteine residue instead of a tyrosine at position 181 and is highly resistant to nevirapine;¹⁶ L100I + K103N, a double mutant RT that carries an isoleucine instead of a leucine at position 100 and an asparagine instead of a lysine at position 103 and is resistant to efavirenz, another clinically used drug.¹⁵ The single mutation, K103N, was not tested, since this mutation is already included in the double mutant variant that shows higher resistance to efavirenz than K103N alone. Compound **8c** inhibited the wild-type RT as well as the T181C

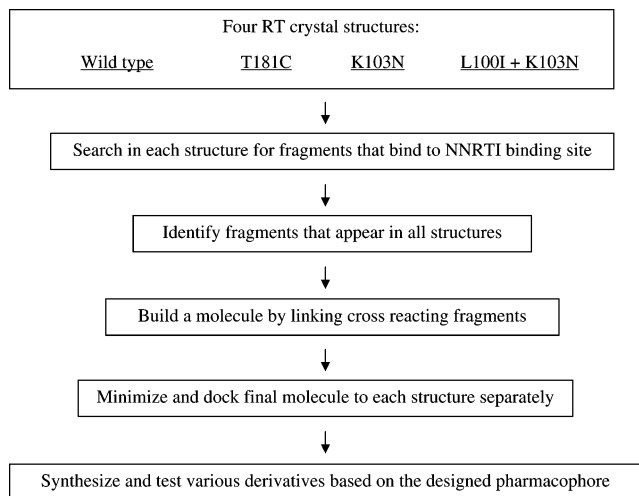


Figure 1. Outline of the design process of new inhibitors against HIV-1 RT.

and L100I-K103N mutants with IC_{50} values of about 9.9, 26, and 20 μM , respectively (Figure 2). This means that **8c** was only about two times less effective in the inhibition of the

mutants compared to the wild type RT. Compound **5f** was even more effective than **8c**, as it inhibited all three RT variants with IC_{50} values below 10 μM and only an ~ 2.7 fold difference in inhibition of the mutant RT, relative to the wild type RT. Compound **5f** was substantially more effective than nevirapine, which inhibited the T181C and the L100I+K103N RT mutants only at IC_{50} values of 100 and 77 μM , respectively, i.e., the mutants had a 45–59 fold increase in resistance to nevirapine (Figure 2). All analyses of the measured data were well fitted to the four-parameter logistic equation with high correlation coefficients (higher than 0.98).

The mode of inhibition of RT-associated DNA polymerase activity by **5f**, the most efficient inhibitor, was further investigated in a DNA polymerase primer-extension assay. In this assay, the RT is allowed to extend a 5'-end-labeled 15-mer primer that was annealed to a ϕX174 single-stranded DNA. The reaction products are then analyzed by urea-PAGE, and as was shown by us previously,²² the length of the DNA products is usually up to about 500nt in length, with several strong pausing sites (Figure 3). The experiments were divided into two sets: in the first one HIV-1 RT was initially preincubated with the inhibitor followed by the addition of the labeled template-primer; in the second, the RT was first preincubated with the template-

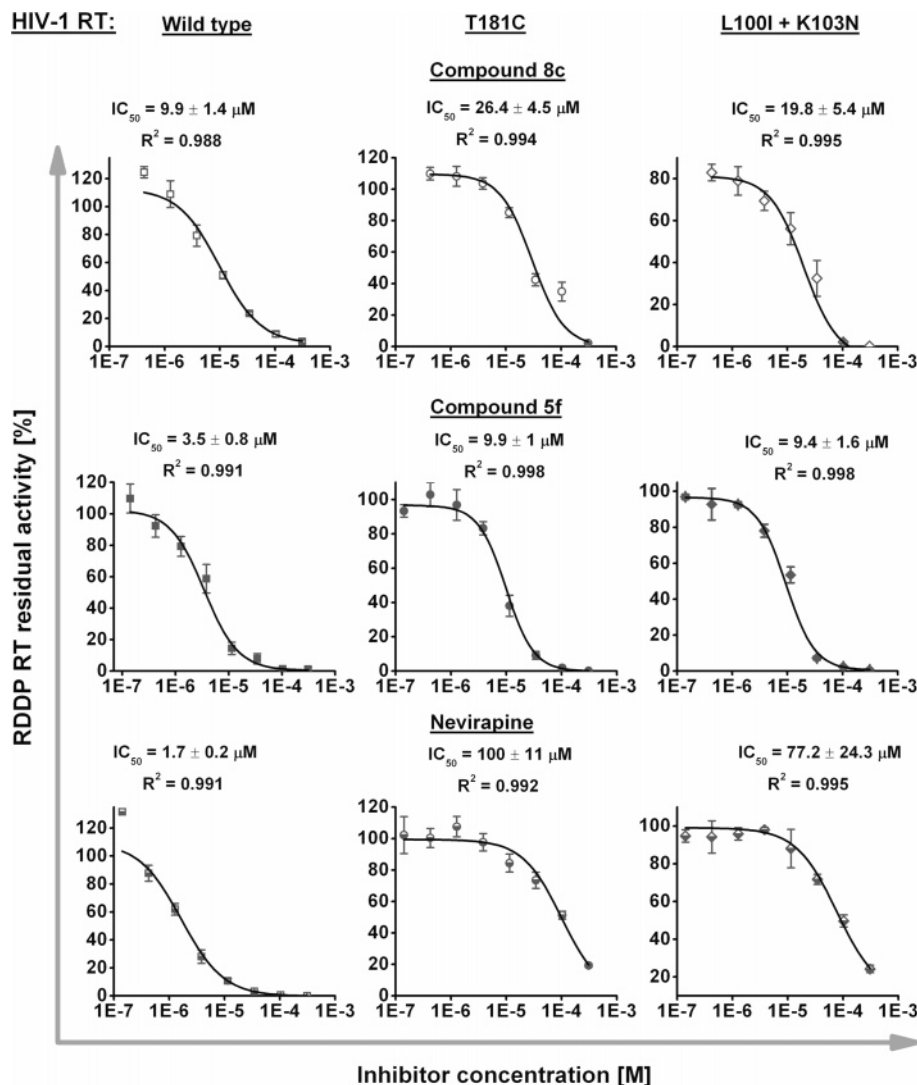


Figure 2. Inhibition of wild type and drug-resistant mutant RTs by compounds **8c** and **5f**. Wild type RT (left column), single mutant T181C RT (middle column), and double mutant RT L100I-K103N (right column) were assayed for DNA polymerase activity in the presence of various concentrations of three compounds: **8c** (top row), **5f** (middle row), and nevirapine (bottom row). The dose–response curves were fitted to a four-parameter logistic equation, and the IC_{50} parameter as well as standard errors and correlation coefficients are reported.

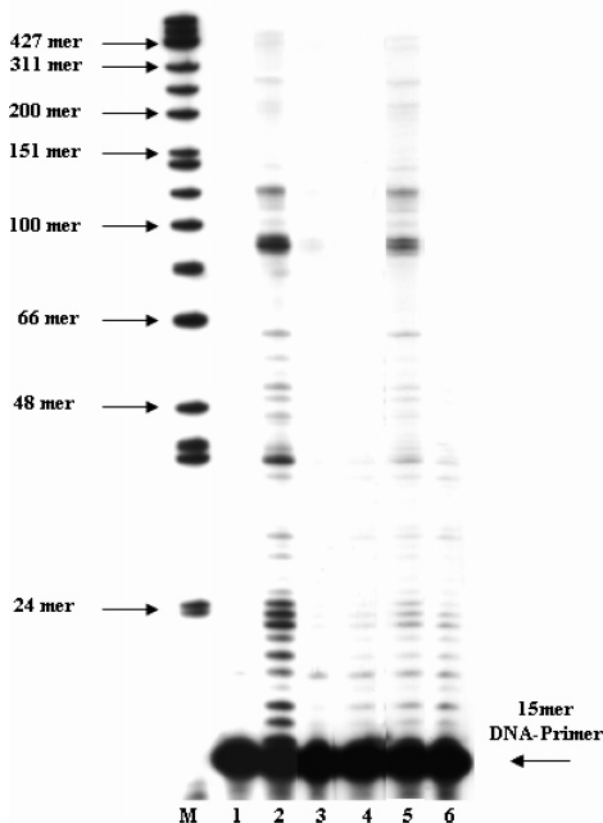


Figure 3. DNA primer extension by HIV-1 RT in the presence of compound **5f** and nevirapine. In all conducted reactions HIV-1 RT was preincubated on ice for 30 min. In lanes 2–4 RT was preincubated with an inhibitor followed by the addition of the template-primer (T/P), and in lanes 5–6 RT was preincubated with T/P followed by addition of the inhibitor. The reactions were initiated with the addition of the relevant substrates and were then further incubated at 37 °C for 30 min. M: DNA molecular size marker. A nonphosphorylated ϕ X174am3 double-stranded DNA, *Hinf*I cut (from Promega) was 5'-end labeled with [γ - 32 P] ATP. Lane 1: T/P only, lane 2: RT without inhibitors, lane 3: RT in the presence of compound **5f**, lane 4: RT in the presence of nevirapine, lane 5: RT in the presence of compound **5f**, after preincubation with the T/P for 5 min on ice, lane 6: RT in the presence of nevirapine, after preincubation with the T/P for 5 min on ice. All reactions included 2% DMSO.

primer followed by the addition of the inhibitor. The primer elongation, obtained in the presence of either **5f** or nevirapine, was strongly impaired when RT was first incubated with the inhibitors (lanes 3 and 4, respectively, compared to lane 2). This inhibition was mostly abolished when the RT was preincubated

with the template-primer prior to the addition of compound **5f** (lane 5 compared to lane 3). On the other hand, the order of adding the reaction components had little effect on the inhibition obtained by nevirapine (lane 6 compared to lane 4).

Compounds **8c** and **5f** were also tested in a gel mobility shift assay for their effects on the formation of RT–DNA complex. In this assay, the DNA is 5'-end labeled with [32 P]ATP and incubated with RT. The amount of the complexed DNA–RT (as well as the free DNA) that formed can be monitored after separating the reaction products by electrophoresis on non-denaturing polyacrylamide gels. As shown in Figure 4, none of the compounds, including the NNRTI inhibitor nevirapine, prevented the binding of RT to the DNA. This conclusion is drawn from the fact that in the case of the two novel molecules the amount of the bound DNA was similar to that detected when RT was incubated with the DNA without any inhibitor. In contrast to compounds **8c** and **5f**, 1,4-benzenediol, 2-[[[(1R,2R,5S,8aS)-1,2,3,5,6,7,8,8a-octahydro-1,2,5-trimethyl-5-[2-[(1R,2S,4aR)-1,2,3,4,4a,5,6,7-octahydro-1,2,5,5-tetramethyl-1-naphthalenyl]ethyl]-1-naphthalenyl]methyl], bis(hydrogen sulfate) (toxiusol), a natural product that was shown by us to be a potent RT inhibitor,²³ prevented the binding of the enzyme to DNA and was used as a positive control.

The thirteen most effective molecules (Table 3) were also tested for their cytotoxic effects on Jurkat cells, using the XTT assay that measures cell death (see Experimental Section). In this assay, none of the tested molecules showed any substantial effect on the viability of the cells. Seven of them were not toxic at the tested concentrations, while the other six showed moderate toxicity, with CC₅₀ values in the range of 213–251 μ M (Table 3).

Discussion

On the basis of the known various crystal structures of HIV-1 RT, we designed *in silico* a molecule that is capable of binding to both wild type and drug-resistant mutant RTs. The molecule was used as a scaffold for the synthesis of various compounds, and 27 of them were tested for their ability to inhibit the DNA polymerase activity of RT. More than 50% of the tested compounds displayed a significant capacity to inhibit the RT activity with apparent IC₅₀ values below 100 μ M, out of which 29% demonstrated IC₅₀ values below 10 μ M. This undoubtedly shows that the collection of novel molecules was enriched for their capacity to inhibit RT. Moreover, this hit rate of active molecules is significantly higher than the proportion expected from a high throughput screening of a random list of compounds.

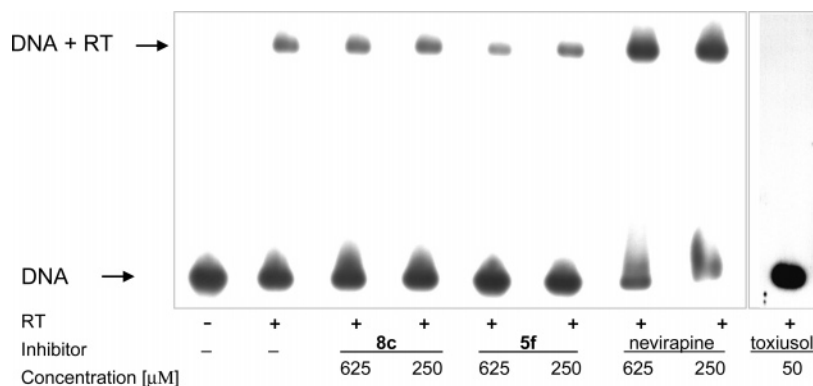


Figure 4. The effect of compounds **8c**, **5f**, and nevirapine on the formation of RT–DNA complex. The PAGE mobility shift assay was performed as described in the Experimental Section. The lanes in the autoradiogram are of the following reactions: lane 1, control with no RT present; lane 2, binding in the absence of inhibitors; lanes 3–8, binding in the presence of compounds **8c**, **5f**, and nevirapine at the indicated concentrations. Lane 9, positive control, of binding in the presence of toxiusol.

The parallel screen of small fragments against various structures of RT successfully led to several effective inhibitors. This novel method had several advantages. First, it enabled filtering molecules that could interact with the wild type and mutant variants. Second, it took into account subtle movements of residues in the different structures that might represent a better description of the binding site in the RT conformation. Third, several cycles of docking into different structures was presumably more reliable than only a single docking into a specific RT structure. Therefore, it was expected to increase the proportion of true binders and to decrease the proportion of false positive binders.

The computational approach presented in this study could serve as an alternative or complementary tool to other fragment-based methods, such as NMR or functional assay screenings at high compound concentrations, both of which have gained increasing popularity during recent years.^{24–27} While application of the computational approach is purely theoretic, it can be easily used to screen a huge amount of compounds, sampling a wide range of the chemical space encompassed by all the possible molecules. Yet, any potential compound has to be tested *in vitro* for confirming its inhibition or binding effects on the target protein. On the other hand, screening fragments by NMR or functional assays represent experimental techniques intended to isolate specific fragments interacting with a target protein. NMR has low false positive hits and high sensitivity and gives some information on the binding mode (but no confirmation for actual inhibitory activity), while only functional assays can validate the inhibitory nature of the compounds.²⁴ Nevertheless, both techniques are limited by the number of the substances that can be tested, and the solubility of the fragments that have to be tested at high concentrations. Evidently, computational methods can complement any of these experimental methods by preselecting potential fragments for the experimental screen or by aiding the optimization and linkage of the fragments isolated.

Incorporation of halogens in the inhibitor has been shown in various examples to notably improve the inhibition of RT. Efavirenz, which is the most potent inhibitor currently used nowadays in clinical treatment, has a chlorine and a trifluoromethyl group. Masuda et al. demonstrated that the effectiveness of several RT inhibitors was significantly improved upon substitution by halogens and NO₂.⁹ Therefore, it is not surprising that addition of halogens in compounds **8c** and **6a** led to a dramatic increase in the efficacy of the inhibition. This effect is probably due to the overall combination of the constituents and the molecular orientation of the functional groups in the molecule rather than to the presence of the halogens since in the iodine-containing **10a** no inhibitory effect was detected. Interestingly, the same improved inhibitory effect was observed after the addition of a chlorine in compound **5b** and a benzoyl group in compound **5d**; both molecules contain 2-oxopropanenitrile groups and showed a marked inhibition of RT compared to the other molecules with the same 2-oxopropanitrile group.

The most efficient inhibitors were further tested for their capacity to inhibit the RNase H activity of RT, and all of them showed higher IC₅₀ values than the values measured for inhibition of the DNA polymerase activity. This difference was mostly prominent with molecules, such as **6a** and **5d**. Other compounds, such as **8c**, **5b**, and **5f**, inhibited both RT-associated activities with about 4- to 7-fold reduced inhibition efficacy of the RNase H activity compared to the DNA polymerase activity (Table 3). These results suggest that these broad range inhibitors might have various modes of binding leading to inhibition of

the RT, since the catalytic domains for the DNA polymerase and RNase H are located in different domains of RT (although there are tight interactions between these two domains, and many mutations affect both RT activities).²⁸

Both activities of RT were inhibited most effectively by compound **5f**, which was only slightly cytotoxic to Jurkat cells with a CC₅₀ of 247 μM (Table 3). This compound showed an improved profile against drug-resistant mutants compared to nevirapine. Compound **5f** inhibited the DNA polymerase activity of wild type RT slightly less effectively than nevirapine (by 2-folds). More importantly, **5f** inhibited more effectively than nevirapine the T181C mutant and the L100I-K103N double mutant RTs by 10- and 8-fold, respectively (Figure 2).

Interestingly, the additional methylene in compound **5f** compared to **5a** (by replacing the 2-oxopropanenitrile with 2-oxobutanitrile) had a drastic effect on its ability to inhibit RT. While **5a** did not inhibit RT at all, the additional methylene rendered compound **5f** to be a highly potent inhibitor against RT. This might be due to steric hindrance of **5a** inside the hydrophobic pocket within the RT or to greater flexibility or accessibility of **5f**.

DNA-primer extension experiments showed that the prior binding of the template-primer to RT before interaction of RT with **5f** mostly abrogates the inhibition of RT (see Figure 3, lane 5 compared to lane 3). In addition, compound **5f** did not prevent the formation of DNA–RT complexes, as evident from the gel shift assay (Figure 4). In all, it is likely that **5f** did not alter the binding of RT to DNA, but formation of the RT–DNA complex interfered substantially with the interaction of the inhibitor with RT. This pattern of inhibition could be explained if the conformational changes of the RT, induced by binding of the template-primer to RT, could obstruct inhibitor binding. Alternatively, binding of the DNA to RT might partially obscure free access of the inhibitor to its binding site. In light of this behavior as well as the effective inhibition of the drug-resistant RT variants, it seems that **5f** inhibits RT by a different mechanism from that of nevirapine.

Docking of compounds **5f** and **8c** into the HIV-1 RT structure (Figure 5) showed that they both fit well into the NNRTI binding pocket. In both molecules the phenyl group is positioned in the vicinity of Trp 229, Tyr 188, and Tyr 181 residues of RT (located in the p66 subunit), while other functional groups of the compounds are extended to interact with other residues in the hydrophobic pocket of RT. According to this model, **8c** formed H-bonds with both Lys 101 and His 235 residues of the p66 subunit of RT (Figure 5a). One bond was formed between the backbone carbonyl of Lys 101 and the hydrogen of the NH group in the imidazole ring, and a second bond was formed between the backbone carbonyl of His 235 and the hydrogen of the amide group of **8c**. This model is supported by the experimentally observed interaction of NNRTI inhibitors³ with Lys 101. Compound **5f** formed one H-bond between the ketone group of the compound and the hydroxyl group of the side chain of Tyr 318, located in the p66 subunit of RT (Figure 5b). Since **5f** formed fewer H-bonds with RT than **8c** but inhibited the enzyme more efficiently, it may have a more favorite hydrophobic interaction with RT than **8c**.

Of the molecules studied, **8c**, **5d**, **5b**, and **5f** were the most effective against HIV-1 RT enzymatic activities, and all four of them have drug-like properties (Table 4). Their molecular weight ranges from 179.6 to 300.5, and they have between two and four H-bond acceptor atoms and between zero and three H-bond donor atoms. The LogP values of the molecules range from 1.6 to 2.4, and they have no more than four rotatable bonds.

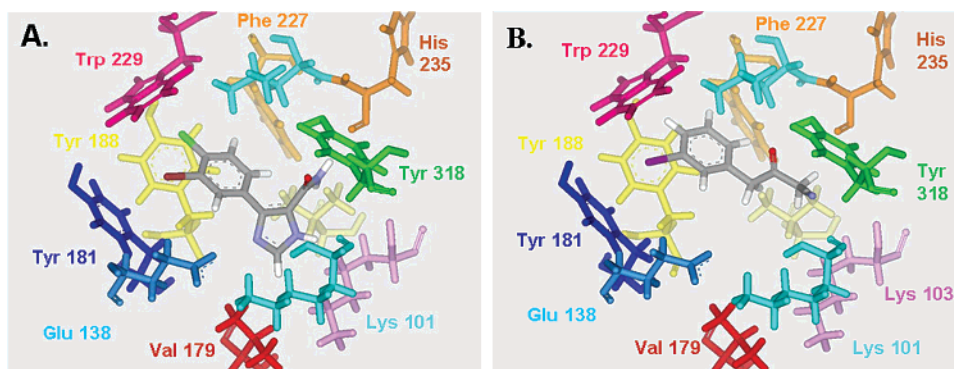


Figure 5. Docking compounds **8c** and **5f** into the NNRTI binding site of the wild type RT. **8c** (A) and **5f** (B) were docked into the structure of RT found in PDB entry 1fkp using surflex software. The top scored conformation of each molecule is shown. Amino acids in the pocket are specified in three-letter codes and different colors, Glu 138 is part of the p51 subunit, and all the other amino acids are part of the p66 subunit. The two compounds are depicted in CPK (Corey, Pauling, and Kulin) colors and are displayed as a stick model.

Table 4. Molecular Properties of the Most Efficient Inhibitors of HIV-1 RT

compd	mol weight	H-bond donors	H-bond acceptors	miLogP ^a	TPSA ^b	rotatable bonds
5b	179.6	0	2	1.572	40.9	2
5d	249.3	0	3	2.349	57.9	4
5f	285.1	0	2	1.802	40.9	3
8c	300.5	3	4	2.072	71.8	2

^a Molinspiration calculated LogP. ^b Topological polar surface area [Å²].

In addition, the polar surface area of all of them is less than 60 Å² which is a good indication for bioavailability.²⁹ None of the four molecules violates any of the Lipinski rule of 5,³⁰ and therefore they represent attractive compounds for further research. These substances are currently under further development and will be tested in the future for their capacity to inhibit HIV in a cell-based assay.

Experimental Section

Molecular Modeling. The RT structures 1fkp, 1fko, and 1jkh were downloaded from the Research Collaboratory for Structural Bioinformatics site (<http://www.rcsb.org/pdb>) as a complex with efavirenz and were saved as pdb files. 1fkp is the structure of a wild type RT with a resolution of 2.5 Å, 1fko carries the mutation K103N and has a resolution of 2.9 Å and 1jkh carries the mutation T181C and has a resolution of 2.5 Å. All structures were modified with the Cerius 2 software as follows: first the inhibitor and water molecules were removed. The structures were then inspected for the correct double bonds, hydrogen atoms were added to each structure, and only these atoms were energy minimized with the CFF 1.02 force field. The double mutant K103N + L100I is not found in the protein database, and its structure was generated by replacing leucine 100 in the 1fko structure with isoleucine and then minimizing the energy of the amino acid, using the CFF 1.02 force field.

A scaffold inhibitor molecule was designed by using the Ludi module of the Cerius 2 software (Accelrys inc. <http://www.accelrys.com>). The center of the NNRTI binding site in each structure was defined based on the amino acid residues that form the binding site, and a *de novo* search with a radius of 10 Å was initiated with a library of 1000 fragments. The bond rotation parameter was set to one at a time to allow flexibility to the search, and the search type parameter was set to best. Fragments that interacted with the binding site were scored with the energy_estimate_3 scoring function³¹ (that includes aromatic–aromatic interactions in addition to the other terms) and were averaged over all structures. From the top scored fragments the phenyl and trimethylpyrrole fragments were repositioned in the binding site of all structures, and a second search in a link mode (double links) was initiated. This search looks for fragments that could link the phenyl to the trimethylpyrrole,

and it suggested linking the two groups through another phenyl group. The resulting molecule was subjected to another link mode (single links) search, in which an amide group was added to the pyrrole ring.

Docking of molecules to the NNRTI binding site of all RT structures was performed with the module ligand fit within Cerius 2 module.²⁰ The docking site was generated with the site search function, based on the bond inhibitor efavirenz (before its deletion from the structure), with the opening size parameter set to 5 Å and the resolution parameter to 0.5 Å. The molecule was energy minimized using the CFF1.02 field force and then docked into the NNRTI binding site using the following parameters: flexible fit, number of trials = 150000, maximal number of conformations = 4, search step for torsions w/polar hydrogen = 5 degrees, saved only diverse conformers (rms thresholds = 1.5 Å), energy minimized ligands in the protein and PLPv.1 energy grid. The final docking poses were scored with Ligscoere1 and PLP2 scoring functions (negative values of PLP2 function were replaced with positive ones for consistency).

Docking of compounds **8c** and **5f** into RT was performed with the Surfex software.³² The original inhibitor in structure 1fkp was used to generate a protomol, an idealized binding site ligand, using the defaults setting of the program. For each compound, the charge was calculated, and the structure was energy minimized and then docked into 1fkp structure using the generated protomol. Surfex docks the molecules by fragmentation each one and fitting each conformation of each fragment to the protomol to yield poses that maximize molecular similarity to the protomol. The docked conformation with the highest score, for each molecule, was selected and analyzed visually with Discovery studio visualizer 1.6 (Accelrys software inc.).

The molecular properties of the best inhibitors were calculated with the molinspiration on-line calculator (<http://www.molinspiration.com/cgi-bin/properties>).

Chemistry. General. ¹H and ¹³C NMR spectra were obtained on 200, 300, and 600 MHz Bruker AC-200, AM-300, and DMX-600 spectrometers. Chemical shifts are expressed in ppm downfield from Me₄Si used as internal standard. The values are given in δ scale. Mass spectra were obtained on a Varian Mat 731 spectrometer. HRMS were obtained on a VG AutoSpec E spectrometer. The reaction progress was monitored by TLC on silica gel (Merck, Art. 5554) or alumina. (Riedel-de Haen, Art. 37349). Flash chromatography was carried out on silica gel (Merck, Art. 9385). Commercially available compounds were used without further purification.

3-(2-Bromoacetyl)phenyl Diethyl Phosphate (2).³³ Diethyl chlorophosphate (1.39 mmol, 0.2 mL) and triethylamine (1.16 mmol, 0.16 mL) were added in sequence to a stirred solution of **1** (1.16 mmol 0.25 g) in anhydrous CH₂Cl₂ (25 mL). The obtained solution was stirred at room temperature for 3 h followed by addition of distilled water. The organic phase was separated, washed with brine, and dried over MgSO₄. The filtrate was evaporated to

give brown colored oil. Upon addition of ether, a brown solid was obtained and removed. The yellow ethereal solution was evaporated, and the residue was purified by column chromatography ($\text{CH}_2\text{Cl}_2/\text{EtOAc} = 20:1$) to provide **2** as a colorless oil in 43% yield. ^1H NMR (300 MHz, acetone- d_6) δ 7.92–7.84 (m, 2H, *H*-C4, *H*-C6), 7.62 (t, 1H, *J* = 7.2 Hz, *H*-C5), 7.56–7.53 (m, 1H, *H*-C2), 5.05 (s, 2H, CH_2Br), 4.23 (AB sys of qd, 1H, *J* = 10; 8; 7 Hz, CH_2Me), 1.33 (td, 6H, *J* = 7.2; 1.2 Hz, CH_2CH_3). ^{13}C NMR (300 MHz, acetone- d_6 , where applicable *J*, in Hz, are given in parentheses) δ 191.1 (*CO*), 152.15 (C3, d, *J* = 6 Hz), 137.05 (C1), 131.2 (C5), 126.1 (C4, d, *J* = 4.5 Hz), 125.9 (C6), 120.4 (C2, d, *J* = 4.5 Hz), 65.2 (CH_2Me , d, *J* = 6 Hz), 47.5 (CH_2Br), 16.4 (CH_2CH_3 , d, *J* = 6.5 Hz). ^{31}P NMR (81.01 MHz, acetone- d_6) δ -5.85 (broad quint, *J* = 8 Hz). MS (CI+) *m/z*: 257.057 ([*M* - CH_2Br], 100), 352.999 (MH^+ , 30). HRMS: calcd for $\text{C}_{12}\text{H}_{17}\text{O}_5\text{BrP}$ (MH^+ , CI+) 352.9977 found 352.9986.

3-Phenyl-benzoic Acid (3e).³⁴ To a solution of NaOH (0.048 mol), 3-iodobenzoic acid **3a** (0.024 mol), and phenylboronic acid (0.026 mol) in H_2O (100 mL) was added $\text{Pd}(\text{OAc})_2$ (5% mol), and the colorless mixture was stirred at room temperature for 2 h, while at the end it turned to a black colored solution. The solution was acidified with 1N HCl and extracted with EtOAc. The organic phase was washed with brine, dried over MgSO_4 , and filtered through a celite bed. The colorless filtrate was evaporated to give **3e** as a white solid in quantitative yield; mp 155–157 °C [lit.³⁴ 112–114 °C]. ^1H NMR (300 MHz, DMSO- d_6) δ 8.2–8.15 (t, 1H, *J* = 1.9 Hz, *H*-C2), 7.96–7.9 (m, 2H, *H*-C4, *H*-C6), 7.71–7.68 (m, 2H, *Ph*), 7.62–7.57 (t, 1H, *J* = 7.8 Hz, *H*-C5), 7.51–7.46 (m, 2H, *Ph*), 7.42–7.37 (m, 1H, *Ph*). ^{13}C NMR (300 MHz, DMSO- d_6) δ 167.66 (*CO*), 142.18 (*Ph*), 140.82 (C3), 132.19 (C4), 130.0 (C2), 129.87 (C6), 129.68 (C1), 129.31 (C5), 128.77 (*Ph*), 128.65 (*Ph*), 127.79 (*Ph*). MS (CI+) *m/z*: 198.064 (M^+ , 100). HRMS: calcd for $\text{C}_{13}\text{H}_{10}\text{O}_2$ (M^+ , CI+) 198.0681 found 198.0637. Anal. calcd for ($\text{C}_{13}\text{H}_{10}\text{O}_2 \cdot 0.3\text{H}_2\text{O}$): C 76.68, H 5.25; Found: C 76.99, H 5.02.

General Procedure for the Synthesis of Aroyl Chlorides.³⁵ The known aroyl halides **4a–e** were prepared by treatment of the corresponding acids with an excess of SOCl_2 at reflux over night. The excess SOCl_2 was removed, and the residual aroyl halides, obtained in quantitative yield, were isolated as oils or crystals. The products were used without further purification.

3-Iodobenzoyl Chloride (4a).³⁶ Compound **4a** was obtained as a colorless oil from 3-iodobenzoic acid **3a**. ^1H NMR (300 MHz, CDCl_3) δ 8.46–8.45 (td, 1H, *J* = 1.8; 0.6 Hz, *H*-C2), 8.13–8.1 (ddd, 1H, *J* = 7.8; 1.8; 1.79 Hz, *H*-C6), 8.05–8.02 (ddd, 1H, *J* = 7.8; 1.8; 1.79 Hz, *H*-C4), 7.32–7.27 (td, 1H, *J* = 7.8; 0.6 Hz, *H*-C5). ^{13}C NMR (300 MHz, CDCl_3) δ 167.03 (*CO*), 144.09 (C4), 139.84 (C2), 134.92 (C1), 130.55 (C6), 130.51 (C5), 94.2 (C3).

3-Chlorobenzoyl Chloride (4b).³⁷ Compound **4b** was obtained as a colorless oil from compound **3b**. ^1H NMR (200 MHz, acetone- d_6) δ 8.08–8.02 (m, 2H, *H*-C2, *H*-C6), 7.84–7.78 (ddd, 1H, *J* = 8.2; 1.8; 1.3 Hz, *H*-C4), 7.69–7.6 (td, 1H, *J* = 8.2; 0.72 Hz, *H*-C5). ^{13}C NMR (200 MHz, acetone- d_6) δ 167.5 (*CO*), 136.36 (C4), 135.8 (C1, C3), 131.82 (C2), 131.32 (C5), 130.47 (C6).

3-Bromo-4-chlorobenzoyl Chloride (4c).³⁸ Compound **4c** was obtained as a white solid from compound **3c**. ^1H NMR (200 MHz, acetone- d_6) δ 8.34–8.33 (d, 1H, *J* = 2.18 Hz, *H*-C2), 8.13–8 (dd, 1H, *J* = 8.5; 2.18 Hz, *H*-C6), 7.84–7.8 (d, 1H, *J* = 8.5 Hz, *H*-C5). ^{13}C NMR (300 MHz, acetone- d_6) δ 166.65 (*CO*), 142.7 (C1), 136.57 (C2), 133.81 (C4), 132.15 (C6), 132.12 (C5), 123.63 (C3).

3-Benzoyl-benzoyl Chloride (4d).³⁹ Compound **4d** was obtained as a white solid from compound **3d**. ^1H NMR (300 MHz, acetone- d_6) δ 8.47–8.45 (m, 1H, *H*-C2), 8.41–8.36 (m, 1H, *H*-C6), 8.2–8.16 (m, 1H, *H*-C4), 7.87–7.8 (m, 3H, *Ph*, *H*-C5), 7.71–7.68 (m, 1H, *Ph*), 7.61–7.56 (m, 2H, *Ph*). ^{13}C NMR (300 MHz, acetone- d_6) δ 195 (*CO*), 167 (*COCl*), 139 (C3), 137 (*Ph*), 136.39 (C4), 134.42 (C6), 133.2 (C1), 133.08 (*Ph*), 132.01 (C2), 129.86 (*Ph*), 129.75 (C5), 128.67 (*Ph*).

3-Phenylbenzoyl Chloride (4e).⁴⁰ Compound **4e** was obtained as colorless oil from compound **3e**. ^1H NMR (300 MHz, CDCl_3) δ 8.4–8.38 (t, 1H, *J* = 1.62 Hz, *H*-C2), 8.19–8.14 (ddd, 1H, *J* = 7.74; 1.62; 1.21 Hz, *H*-C6), 7.97–7.93 (ddd, 1H, *J* = 7.74; 1.62;

1.21 Hz, *H*-C4), 7.7–7.48 (m, 6H, *Ph*, *H*-C5). ^{13}C NMR (300 MHz, CDCl_3) δ 168.44 (*CO*), 142.25 (*Ph*), 139.19 (C3), 133.93 (C4), 133.82 (C1), 130.18 (C2), 129.86 (C6), 129.49 (C5), 129.147 (*Ph*), 128.31 (*Ph*), 127.18 (*Ph*).

2-(3-Iodophenyl)acetyl Chloride (4f).⁴¹ Compound **3f** (1 mmol) and oxalyl chloride (2 mmol) were dissolved in anhydrous CH_2Cl_2 to which 1 drop of DMF was added. The final solution was stirred at room temperature for 2 h and then concentrated under vacuum to give **4f** as a yellow solid which was used without further purification. ^1H NMR (300 MHz, CDCl_3) δ 7.67 (d, 1H, *J* = 7.7 Hz, *H*-C4), 7.63 (s, 1H, *H*-C2), 7.23 (d, 1H, *J* = 7.7 Hz, *H*-C6), 7.09 (t, 1H, *J* = 7.7 Hz, *H*-C5), 4.08 (s, 2H, CH_2CO). ^{13}C NMR (300 MHz, CDCl_3) δ 171.61 (*CO*), 138.4, 137.3 (C2 and C4), 133.56 (C1), 130.8, 129.0 (C5 and C6), 94.95 (C1), 52.32 (CH_2CO).

General Procedure for the Synthesis of Cyanoacetnitriles 5a–f.⁴² To a cooled (–78 °C) solution of cyanoacetic acid (15 mmol) in anhydrous THF (40 mL) was added *n*-BuLi (2.5 M, 30 mmol, 12 mL) dropwise, and the resulting mixture was stirred for 15 min followed by dropwise addition of an aroyl chloride (7.5 mmol). The mixture was stirred at –78 °C for 1 h and then for an additional 1 h at room temperature, poured into ice–water, and washed with ether, and the organic phase was removed. The aqueous phase was acidified with 1 N HCl and washed twice with ether, the combined organic phase was washed with saturated NaHCO_3 and brine, dried with MgSO_4 , filtered, and evaporated to provide the desired compound.

3-(3-Iodophenyl)-3-oxopropanenitrile (5a).⁴³ Compound **5a** was obtained as a yellow solid from **4a** in 60% yield; mp 105–106 °C. ^1H NMR (300 MHz, CDCl_3) δ 8.24–8.23 (t, 1H, *J* = 1.5 Hz, *H*-C2), 8–7.96 (ddd, 1H, *J* = 7.8; 1.8; 1.2 Hz, *H*-C6), 7.88–7.85 (ddd, 1H, *J* = 7.8; 1.8; 1.2 Hz, *H*-C4), 7.29–7.24 (t, 1H, *J* = 7.8 Hz, *H*-C5), 4.06 (s, 2H, CH_2). ^{13}C NMR (300 MHz, CDCl_3) δ 185.8 (*CO*), 144.44 (C4), 137.27 (C2), 135.82 (C1), 130.72 (C6), 127.49 (C5), 113.27 (*CN*), 94.73 (C3), 29.37 (CH_2). MS (CI+) *m/z*: 230.93 ([*M* - CH_2CN], 100), 270.947 (M^+ , 30). HRMS: calc. for $\text{C}_9\text{H}_6\text{NOI}$ (M^+ , CI+) 270.9494 found 270.9472. Anal. calcd for ($\text{C}_9\text{H}_6\text{INO}$): C 39.88, N 5.17, H 2.23; Found: C 39.75, N 5.21, H 2.19.

3-(3-Chlorophenyl)-3-oxopropanenitrile (5b).⁴⁴ Compound **5b** was obtained as a white solid from **4b** in 68% yield; mp 73 °C. ^1H NMR (300 MHz, CDCl_3) δ 7.9–7.88 (td, 1H, *J* = 2.1; 0.3 Hz, *H*-C2), 7.81–7.77 (ddd, 1H, *J* = 7.8; 1.5; 0.9 Hz, *H*-C6), 7.65–7.61 (ddd, 1H, *J* = 7.8; 2.1; 0.9 Hz, *H*-C4), 7.5–7.43 (td, 1H, *J* = 7.8; 0.6 Hz, *H*-C5), 4.09 (s, 2H, CH_2). ^{13}C NMR (600 MHz, CDCl_3) δ 186.06 (*CO*), 135.66 (C1), 135.59 (C3), 134.67 (C4), 130.47 (C2), 128.46 (C6), 126.5 (C5), 113.32 (*CN*), 29.54 (CH_2). MS (CI+) *m/z*: 138.98 ([*M* - CH_2CN], 100), 180.02 (MH^+ , 10). HRMS: calc. for $\text{C}_9\text{H}_7\text{NOCl}$ (M^+ , CI+) 180.0216 found 180.0199. Anal. calcd for ($\text{C}_9\text{H}_6\text{ClNO} \cdot 0.1\text{H}_2\text{O}$): C 59.59, N 7.72, H 3.44; Found: C 59.45, N 7.93, H 3.38.

3-(3-Bromo-4-chlorophenyl)-3-oxopropanenitrile (5c). Compound **5c** was obtained as a white solid from **4c** in 58% yield; mp 95–98 °C. ^1H NMR (300 MHz, CDCl_3) δ 8.4–8.13 (d, 1H, *J* = 2.1 Hz, *H*-C2), 7.79–7.76 (dd, 1H, *J* = 8.4; 2.1 Hz, *H*-C6), 7.6–7.57 (d, 1H, *J* = 8.4 Hz, *H*-C5), 4.1 (s, 2H, CH_2). ^{13}C NMR (300 MHz, CDCl_3) δ 184.97 (*CO*), 141.68 (C1), 133.66 (C4, C2), 131.1 (C6), 127.99 (C5), 123.84 (C3), 113.02 (*CN*), 29.41 (CH_2). HRMS: calcd for $\text{C}_9\text{H}_5\text{NOBrCl}$ (M^+ , CI+) 258.9214 found 258.9217. Anal. calcd for ($\text{C}_9\text{H}_5\text{BrClNO} \cdot 0.2\text{C}_4\text{H}_{10}\text{O}$): C 43.06, N 5.12, H 2.58; Found: C 43.24, N 5.39, H 2.17.

3-Benzoyl-3-oxopropanenitrile (5d). Compound **5d** was obtained as a yellow solid in 54% yield from **4d**; mp 125–128 °C. ^1H NMR (300 MHz, acetone- d_6) δ 8.37–8.36 (td, 1H, *J* = 1.8; 0.3 Hz, *H*-C2), 8.31–8.27 (ddd, 1H, *J* = 7.8; 1.8; 1.2 Hz, *H*-C6), 8.09–8.06 (ddd, 1H, *J* = 7.8; 1.8; 1.2 Hz, *H*-C4), 7.84–7.67 (m, 4H, *Ph*, *H*-C5), 7.61–7.55 (m, 2H, *Ph*), 4.69 (s, 2H, CH_2). ^{13}C NMR (300 MHz, acetone- d_6) δ 194.72 (*CO*), 188.47 (*COCH}_2\text{CN}*), 138.32 (C3), 136.93 (*Ph*), 134.77 (C4), 133.84 (C1), 132.94 (C6), 131.82 (C2), 129.84 (*Ph*), 129.26 (*Ph*), 128.26 (C5), 114.51 (*CN*), 29.49 (CH_2). MS (CI+) *m/z*: 209.064 ([*M* - CH_2CN] $^+$, 100),

249.072 (M^+ , 40). HRMS: calcd for $C_{16}H_{11}NO_2$ (M^+ , CI^+) 249.0790 found 249.0768.

3-Phenyl-3-oxopropanenitrile (5e). Compound **5e** was obtained as a white solid in 15% yield from **4e**; mp 85–87 °C. 1H NMR (300 MHz, $CDCl_3$) δ 8.13–8.12 (t, 1H, $J = 1.8$ Hz, $H-C2$), 7.88–7.83 (dd, 2H, $J = 7.9$; 1.8 Hz, $H-C6$, $H-C4$), 7.6–7.57 (m, 2H, Ph), 7.51–7.41 (m, 4H, Ph , $H-C5$), 4.1 (s, 2H, CH_2). ^{13}C NMR (300 MHz, $CDCl_3$) δ 187.25 (CO), 142.58 (Ph), 133.48 ($C4$), 132.45 ($C3$), 129.93 ($C2$), 129.21 ($C6$), 129.06 ($C5$), 128.35 (Ph), 127.97 ($C1$), 127.3 (Ph), 127.23 (Ph), 113.89 (CN), 29.65 (CH_2). MS (CI^+) m/z : 181.066 ($[M - CH_2CN]^+$, 100), 221.086 (M^+ , 55). HRMS: calcd for $C_{15}H_{11}NO$ (M^+ , CI^+) 221.0841 found 221.0857.

4-(3-Iodophenyl)-3-oxobutanenitrile (5f). Compound **5f** was obtained as a cream colored solid in as a 78% yield from **4e**; mp 96–98 °C. 1H NMR (300 MHz, acetone- d_6) δ 7.65 (m, 2H, $H-C2$, $H-C4$), 7.28 (d, 1H, $J = 7.8$ Hz, $H-C6$), 7.14 (t, 1H, $J = 7.8$ Hz, $H-C5$), 4.02, 3.98 (s, s, 4H, $Ph-CH_2$, CH_2CN). ^{13}C NMR (300 MHz, acetone- d_6) δ 196.8 (CO), 139.6 ($C2$), 137.1 ($C1$), 136.9 ($C3$), 130.27 ($C6$ and $C5$), 115.2 (CN), 48.0 ($Ph-CH_2$), 29.6 (CH_2CN). MS (CI^+) m/z : 216.937 ($[M - COCH_2CN]^+$, 65), 284.966 (M^+ , 25). HRMS: calcd for $C_{10}H_8NOI$ (M^+ , CI^+) 284.9651 found 284.9659.

3-(2-Cyanoacetyl)phenyl Diethyl Phosphate (5h).⁴⁵ A solution of KCN (54 mg, 0.83 mmol) in distilled water (a few drops) was added in one portion to a solution of **2** (117 mg, 0.33 mmol) in 95% EtOH (4 mL). The mixture became yellow and was stirred at room temperature for 5 h. The reaction course was followed by TLC, and an additional amount of KCN was added if needed. To the mixture were then added CH_2Cl_2 and water and acidified with glacial acetic acid (pH = 5–6). The organic phase was separated, washed with brine dried over $MgSO_4$, and evaporated. Final purification by column chromatography (eluent $CH_2Cl_2/EtOAc = 10:1$) gave **5h** as a colorless oil in 40% yield. 1H NMR (300 MHz, acetone- d_6) δ 7.86 (m, 1H, $H-C6$), 7.83 (m, 1H, $H-C2$), 7.62 (t, 1H, $J = 8.5$ Hz, $H-C5$), 7.59 (m, 1H, $H-C4$), 4.62 (s, 2H, CH_2Br), 4.23 (AB sys of qd, 1H, $J = 10$; 8; 7 Hz, CH_2Me), 1.32 (td, 6H, $J = 7$; 1 Hz, CH_2CH_3). ^{13}C NMR (300 MHz, acetone- d_6 , where applicable J_{cp} , in Hz, are given in parentheses) δ 188.9 (CO), 152.3 ($C3$), 137.5 ($C1$), 131.3 ($C5$), 126.6 ($C4$, d, $J = 4.5$ Hz), 125.9 ($C6$), 120.4 ($C2$, d, $J = 5$ Hz), 115.33 (CN), 65.3 (CH_2Me , d, $J = 6$ Hz), 30.3 (CH_2Br), 16.3 (CH_2CH_3 , d, $J = 6.5$ Hz). ^{31}P NMR (81.01 MHz, acetone- d_6) δ -5.85 (br quint, $J = 8$ Hz). MS (CI^+) m/z : 257 ($[M - CH_2CN]^+$, 41), 297 (M^+ , 8), 298 (MH^+ , 11). HRMS: calcd for $C_{13}H_{17}NO_3P$ (MH^+ , CI^+) 298.0844 found 298.0869.

General Procedure for the Synthesis of β -Ketoamides 6a–g.⁴⁶ A cyanoacetonitrile **5a–g** (1 mmol) was dissolved in concentrated H_2SO_4 (5 mL) and the solution was stirred at room temperature for 3–5 h and was then poured into ice water, basified with NH_4OH and extracted with EtOAc. The organic phase was washed with brine, dried with $MgSO_4$, filtered and evaporated to provide the desired amide. Some of the compounds were obtained only in a keto form and others as enol-keto mixtures. When the stirring period was reduced most of the products were obtained in the keto form.

3-(3-Iodophenyl)-3-oxopropanamide (6a). Compound **6a** was obtained as a yellow solid in 80% yield from compound **5a**; mp 90–95 °C. 1H NMR (300 MHz, $CDCl_3$) δ 8.35–8.34 (m, 1H, $H-C2$), 8.02–7.93 (m, 2H, $H-C6$, $H-C4$), 7.29–7.24 (t, 1H, $J = 8.5$ Hz, $H-C5$), 7.1–7 (bs, 1H, NH), 6.1–5.8 (bs, 1H, NH), 3.97 (s, 2H, CH_2). ^{13}C NMR (300 MHz, $CDCl_3$) δ 194.12 (CO), 167.79 (CON), 142.83 ($C4$), 137.4 ($C2$), 137.28 ($C1$), 130.52 ($C6$), 127.4 ($C5$), 94.7 ($C3$), 44.91 (CH_2). MS (CI^+) m/z : 164.038 ($[M - I]$, 100), 230.914 ($[M - CH_2CONH_2]$, 30), 289.972 (MH^+ , 40). HRMS: calcd for $C_9H_9NO_2I$ (MH^+ , CI^+) 289.9678 found 289.9718.

3-(3-Chlorophenyl)-3-oxopropanamide (6b).⁴⁷ Compound **6b**, present as a mixture of ketone and enol forms (1:1.9), was obtained as a yellow solid in 80% yield from **5b**; mp 125–130 °C [lit.⁴⁷ 135–137 °C]. 1H NMR (300 MHz, acetone- d_6) δ 8–7.93 (m, 2H, $H-C2(ket)$, $H-C6(ket)$), 7.76–7.74 (m, 1H, $H-C2(enol)$), 7.72–

7.69 (dt, 1H, $J = 6.9$; 2.1 Hz, $H-C6(enol)$), 7.67–7.63 (ddd, 1H, $J = 8.1$; 2.1; 1.2 Hz, $H-C4(ket)$), 7.58–7.53 (t, 1H, $J = 7.8$ Hz, $H-C5(ket)$), 7.49–7.44 (m, 2H, $H-C4(enol)$, $H-C5(enol)$), 7.12 (bs, 1H, $NH(ket/enol)$), 6.68–6.52 (bs, 1H, $NH(ket/enol)$), 5.9 (s, 1H, $CH(enol)$), 3.96 (s, 2H, $CH_2(ket)$). ^{13}C NMR (600 MHz, acetone- d_6) δ 194.12 ($CO(ket)$), 175.47 ($CON(ket)$), 169.02 ($CON(enol)$), 139.52 ($C1(ket)$), 137.55 ($C1(enol)$), 135.12 ($C3(ket)$), 134.99 ($C3(enol)$), 133.77 ($C4(ket)$), 131.26 ($C2(ket)$), 131.18 ($C4(enol)$), 131.13 ($C2(enol)$), 129.1 ($C6(ket)$), 127.94 ($C5(ket)$), 126.2 ($C6(enol)$), 124.78 ($C5(enol)$), 89.73 ($CH(enol)$), 47.42 ($CH_2(ket)$). MS (CI^+) m/z : 197.027; 198.03 (M^+ , 100; 85). HRMS: calcd for $C_9H_8NO_2Cl$ (M^+ , CI^+) 197.0244 found 197.0266.

3-(3-Bromo-4-chlorophenyl)-3-oxopropanamide (6c). Compound **6c** was obtained as a mixture of ketone and enol forms (1:1.7) as a white solid in 78% yield from compound **5c**; mp 90–92 °C. 1H NMR (300 MHz, acetone- d_6) δ 8.32 (m, 1H, $H-C2(ket)$) 8.05 (d, 1H, $J = 1.8$ Hz, $H-C2(enol)$), 8.03–8 (m, 1H, $H-C6(ket)$), 7.8–7.7 (m, 2H, $H-C5(ket)$, $H-C6(enol)$), 7.65–7.63 (d, 1H, $J = 8.4$ Hz, $H-C5(enol)$), 7.7.11 (bs, 1H, $NH(ket/enol)$), 6.67 (bs, 1H, $NH(ket/enol)$), 5.9 (s, 1H, $CH(enol)$), 3.96 (s, 2H, $CH_2(ket)$). ^{13}C NMR (300 MHz, acetone- d_6) δ 193.27 ($CO(ket)$), 175.26 ($CON(ket)$), 168.64 ($CON(enol)$), 137.78 ($C1(ket)$), 136.62 ($C1(enol)$), 135.91 ($C4(ket)$), 134.64 ($C4(enol)$, $C2(ket)$), 131.59 ($C5(ket)$), 131.47 ($C2(enol)$, $C5(enol)$), 129.82 ($C6(ket)$), 126.78 ($C6(enol)$), 123.04 ($C3(ket)$), 122.92 ($C3(enol)$), 90.01 ($CH(enol)$), 47.33 ($CH_2(ket)$). MS (CI^+) m/z : 276.934 (M^+ , 100). HRMS: calcd for $C_9H_7NO_2ClBr$ (M^+ , CI^+) 276.9328 found 276.9343.

3-(3-Benzoylphenyl)-3-oxopropanamide (6d). Compound **6d** was obtained as a mixture of ketone and enol forms (2:1) as a white solid in 75% yield from compound **5d**. 1H NMR (300 MHz, $CDCl_3$) δ 8.37 (m, 1H, $H-C2(ket)$), 8.23–8.18 (d, 1H, $J = 7.5$ Hz, $H-C4(ket)$), 8.15 (m, 1H, $H-C2(enol)$), 8.05–8.03 (d, 1H, $J = 7.5$ Hz, $H-C6(ket)$), 8–7.98 (d, 1H, $J = 7.5$ Hz, $H-C4(enol)$), 7.86–7.83 (d, 1H, $J = 7.5$ Hz, $H-C6(enol)$), 7.8–7.77 (m, 4H, $Ph(enol/ket)$), 7.66–7.59 (m, 4H, $H-C5(enol/ket)$, $Ph(enol/ket)$), 7.54–7.48 (m, 4H, $Ph(enol/ket)$), 7.05 (bs, 1H, $NH(ket)$), 5.85 (bs, 1H, $NH(ket)$), 5.6 (s, 1H, $CH(enol)$), 5.51 (bs, 2H, $NH(enol)$), 4 (s, 2H, $CH_2(ket)$). ^{13}C NMR (300 MHz, $CDCl_3$) δ 195.37 ($CO(ket/enol)$), 194.65 ($CO(ket)$), 171 ($CON(ket)$), 167.74 ($CON(enol)$), 138.46 ($C3(ket)$), 136.84 ($C3(enol)$), 136.24 ($Ph(ket)$), 135.58 ($Ph(enol)$), 134.97 ($C4(ket)$), 134.48 ($C1(ket)$), 134.16 ($C1(enol)$), 133.12 ($C4(enol)$), 132.96 ($C6(ket)$), 132.72 ($C6(enol)$), 132.16 ($C2(enol)$), 131.96 ($C2(ket)$), 131.75 ($C5(enol)$), 129.99 ($Ph(ket/enol)$), 129.61 ($C5(ket)$), 129.36 ($Ph(enol)$), 129.33 ($C-OH(enol)$), 129.07 ($Ph(ket)$), 128.53 ($Ph(ket/enol)$), 87 ($CH(enol)$), 45.24 ($CH_2(ket)$). MS (ES^+) m/z : 268 (MH^+ , 60), 290 (MNa^+ , 50). HRMS: calcd for $C_{16}H_{13}NO_3$ (M^+ , CI^+) 267.0895 found 267.0900.

3-Oxo-3-(3-phenylphenyl)propanamide (6e).⁴⁸ A mixture of amide **6a** (0.34 mmol), phenylboronic acid (0.38 mmol), 2 M aqueous solution of Na_2CO_3 (0.13 g), and $Pd(OAc)_2$ (3.88 mg) in EtOH 95% (10 mL) was refluxed over night and then cooled and filtered through a celite bed. The filtrate was evaporated, and the obtained crude mixture was extracted with EtOAc and $NaHCO_3$. The organic phase was washed with brine, dried over $MgSO_4$ and evaporated to dryness to give **6e** in quantitative yield; mp 95 °C. 1H NMR (600 MHz, $CDCl_3$) δ 8.18 (s, 1H, $H-C2$), 7.93–7.92 (d, 1H, $J = 7.8$ Hz, $H-C6$), 7.8–7.79 (d, 1H, $J = 7.8$ Hz, $H-C4$), 7.58–7.56 (m, 2H, Ph), 7.46–7.42 (m, 3H, Ph), 7.38–7.35 (t, 1H, $J = 7.8$ Hz, $H-C5$), 7.3–7.2 (bs, 1H, NH), 6.3–6.2 (bs, 1H, NH), 4.01 (s, 2H, CH_2). ^{13}C NMR (600 MHz, $CDCl_3$) δ 195.36 (CO), 168.72 (CON), 141.96 ($C1$), 139.68 (Ph), 136.33 ($C3$), 132.62 ($C4$), 129.52 ($C2$), 128.92 (Ph), 127.93 ($C5$), 127.32 ($C6$), 127.1 (Ph), 45.19 (CH_2). MS (CI^+) m/z : 105.035 ($[M - CH_2CONH_2]$, 100), 239.091 (M^+ , 25). HRMS: calcd for $C_{15}H_{13}NO_2$ (M^+ , CI^+) 239.0946 found 239.0907.

3-Oxo-3-phenylpropanamide (6g).⁴⁹ Compound **6g** was obtained from compound **5g** as a white solid in 75% yield. 1H NMR (300 MHz, $CDCl_3$) δ 8–7.98 (d, 2H, $J = 7.5$ Hz, $H-C2$), 7.64–7.46 (m, 3H, $H-C3$, $H-C4$), 3.99 (s, 2H, CH_2). ^{13}C NMR (300 MHz,

CDCl_3) δ 195.56 (CO), 168.87 (CON), 136.16 (C1), 134.02 (C4), 128.82 (C2), 128.54 (C3), 45.36 (CH_2). MS (ES+) m/z : 186 (MNa⁺, 20).

General Procedure for Synthesis of α -Brominated **7a–g**.⁵⁰

A mixture of a ketone (0.65 mmol) and CuBr_2 (0.65 mmol) in anhydrous EtOAc was heated to reflux. The reaction was monitored by TLC, and an additional amount of CuBr_2 was added if needed. The reaction was stopped at the point when no starting material spot was observed, and the mixture was filtered through a short silica column and washed with EtOAc. The filtrate was evaporated and if needed followed by further purification by column chromatography.

2-Bromo-3-(3-iodophenyl)-3-oxopropanamide (7a). Compound **7a** was obtained as a yellow solid in 80% yield from **6a**; mp 93–95 °C. ¹H NMR (300 MHz, CDCl_3) δ 8.24–8.23 (t, 1H, $J = 1.8$ Hz, $H\text{-C}2$), 7.97–7.94 (m, 2H, $H\text{-C}6$, $H\text{-C}4$), 7.27–7.22 (t, 1H, $J = 8.1$ Hz, $H\text{-C}5$), 6.9–6.8 (bs, 1H, NH), 6.25–6.15 (bs, 1H, NH), 5.51 (s, 1H, CH). ¹³C NMR (300 MHz, CDCl_3) δ 189.28 (CO), 166.41 (CON), 143.19 (C1), 138.06 (C2), 135.38 (C4), 130.5 (C6), 128.32 (C5), 94.52 (C3), 43.21 (CH). MS (CI+) m/z : 230.932 ([M – CHBrCONH_2], 100), 368.866 (M⁺, 10). HRMS: calcd for $\text{C}_9\text{H}_7\text{NO}_2\text{I}$ (M⁺, CI+) 368.8684 found 368.8661.

2-Bromo-3-(3-chlorophenyl)-3-oxopropanamide (7b). Compound **7b** was obtained as a yellow solid in 81% yield from **6b**; mp 110–115 °C. ¹H NMR (300 MHz, CDCl_3) δ 7.99–7.98 (t, 1H, $J = 1.8$ Hz, $H\text{-C}2$), 7.9–7.87 (m, 1H, $H\text{-C}4$), 7.62–7.58 (ddd, 1H, $J = 8.1$; 2.1; 0.9 Hz, $H\text{-C}6$), 7.48–7.43 (t, 1H, $J = 7.8$ Hz, $H\text{-C}5$), 6.83 (bs, 1H, NH), 6.17 (bs, 1H, NH), 5.52 (s, 1H, CH). ¹³C NMR (300 MHz, CDCl_3) δ 189.46 (CO), 166.39 (CON), 135.46 (C1), 135.25 (C3), 134.46 (C4), 130.25 (C5), 129.24 (C2), 127.3 (C6), 43.37 (CH). MS (CI+) m/z : 275.939; 277.939 (MH⁺, 84; 100). HRMS: calcd for $\text{C}_9\text{H}_8\text{NO}_2\text{ClBr}$ (MH⁺, CI+) 277.9406 found 277.9387.

2-Bromo-3-(3-bromo-4-chlorophenyl)-3-oxopropanamide (7c). Compound **7c** was obtained as a white solid in 80% yield from **6c**. ¹H NMR (300 MHz, CDCl_3) δ 8.23–8.22 (d, 1H, $J = 2.1$ Hz, $H\text{-C}2$), 7.88–7.84 (dd, 1H, $J = 8.4$; 2.1 Hz, $H\text{-C}6$), 7.57–7.54 (d, 1H, $J = 8.4$ Hz, $H\text{-C}5$), 6.9 (bs, 1H, NH), 6.24 (bs, 1H, NH), 5.49 (s, 1H, CH). ¹³C NMR (300 MHz, acetone- d_6) δ 188.54 (CO), 166.91 (CON), 148.1 (C1), 135.01 (C2, C4), 131.87 (C5), 130.23 (C6), 123.33 (C3), 43.35 (CH).

2-Bromo-3-(3-benzoylphenyl)-3-oxopropanamide (7d). Compound **7d** was obtained as a white solid in 80% yield from **6d**; mp 125–126 °C. ¹H NMR (300 MHz, CDCl_3) δ 8.39–8.38 (t, 1H, $J = 1.28$ Hz, $H\text{-C}2$), 8.23–8.21 (dt, 1H, $J = 7.8$; 1.28 Hz, $H\text{-C}4$), 8.04–8.01 (dt, 1H, $J = 7.58$; 1.28 Hz, $H\text{-C}6$), 7.79–7.76 (m, 2H, Ph), 7.64–7.58 (m, 2H, Ph), 7.51–7.28 (m, $H\text{-C}5$, Ph), 7–6.8 (bs, 1H, NH), 6.15–6 (bs, 1H, NH), 5.6 (s, 1H, CH). ¹³C NMR (300 MHz, CDCl_3) δ 195.4 (CO), 189.77 (CO), 167.08 (CON), 138.34 (C3), 136.67 (Ph), 135.49 (C4), 133.7 (C1), 133.08 (C6), 132.85 (C2), 130.7 (C5), 130.17 (Ph), 129.29 (Ph), 128.67 (Ph), 43.89 (CH). MS (ES+) m/z : 346; 348 (MH⁺, 100; 90). HRMS: calcd for $\text{C}_{16}\text{H}_{13}^{79}\text{BrNO}_3$ (MH⁺, CI+) 346.0079 found 346.0051; $\text{C}_{16}\text{H}_{13}^{81}\text{BrNO}_3$ (MH⁺, CI+) 346.9980 found 346.9998.

2-Bromo-3-(3-phenylphenyl)-3-oxopropanamide (7e). Compound **7e** was obtained from **6e** and was purified by column chromatography (eluent hexane/EtOAc = 2:1) to give **7e** as a yellow solid in 80% yield. ¹H NMR (300 MHz, CDCl_3) δ 8.23–8.22 (t, 1H, $J = 1.8$ Hz, $H\text{-C}2$), 8–7.96 (ddd, 1H, $J = 7.8$; 1.8; 1.2 Hz, $H\text{-C}6$), 7.87–7.83 (ddd, 1H, $J = 7.8$; 1.8; 1.2 Hz, $H\text{-C}4$), 7.62–7.55 (m, 3H, $H\text{-C}5$, Ph), 7.5–7.36 (m, 3H, Ph), 6.9 (bs, 1H, NH), 6.2 (bs, 1H, NH), 5.65 (s, 1H, $CHBr$). ¹³C NMR (300 MHz, CDCl_3) δ 190.82 (CO), 167.05 (CON), 142.36 (C1), 139.74 (Ph), 134.21 (C3), 133.34 (C4), 129.58 (C2), 129.16 (Ph), 128.22 (C5), 128.13 (C6), 128.06 (Ph), 127.33 (Ph), 43.49 ($CHBr$). MS (CI+) m/z : 105.044 ([M – CH_2CONH_2], 80), 239.096 ([M – Br], 20), 317.004 (M⁺, 5).

2-Bromo-3-oxo-3-phenylpropanamide (7 g).⁵¹ Compound **7g** was obtained as a yellow solid in 75% yield by bromination of **6g**; mp 105–108 °C [lit.⁵¹ 124–125 °C]. ¹H NMR (300 MHz, CDCl_3) δ 8.03–8.01 (d, 2H, $J = 7.5$ Hz, $H\text{-C}2$), 7.67–7.62 (t, 1H, $J = 7.5$

Hz, $H\text{-C}4$), 7.54–7.49 (t, 2H, $J = 7.5$ Hz, $H\text{-C}3$), 7–6.9 (bs, 1H, NH), 6.34–6.36 (bs, 1H, NH), 5.59 (s, 1H, $CHBr$). ¹³C NMR (200 MHz, CDCl_3) δ 190.7 (CO), 166.9 (CON), 134.51 (C4), 133.72 (C1), 129.27 (C2), 128.98 (C3), 43.27 (CH). MS (ES+) m/z : 242.244 (MH⁺, 10), 264.266 (MNa⁺, 100).

General Procedure for Brederick Synthesis of Imidazoles **8a–g.**⁵² An α -bromoketone compound **7a–g** (2.61 mmol) was dissolved in formamide (4 mL) followed by addition of 3 drops of concentrated H_2SO_4 . The solution was refluxed at 150 °C for 2 h and was quenched with 1 N Na_2CO_3 . Chloroform was added, and the organic phase was separated, dried over MgSO_4 and evaporated. The crude mixture was further purified by column chromatography (eluent hexane/EtOAc 3:1) to give **8a–g**.

4-(3-Iodophenyl)-1H-imidazole-5-carboxamide (8a). Compound **8a** was obtained as a yellow solid in 5% yield from **7a**. ¹H NMR (300 MHz, CDCl_3) δ 8.57–8.56 (t, 1H, $J = 1.5$ Hz, $H\text{-C}2$), 8.26–8.22 (ddd, 1H, $J = 7.8$; 1.5; 1.4 Hz, $H\text{-C}6$), 7.9 (s, 1H, CH), 7.75–7.7 (ddd, 1H, $J = 7.8$; 1.5; 1.4 Hz, $H\text{-C}4$), 7.18–7.15 (t, 1H, $J = 7.8$ Hz, $H\text{-C}5$), 6.35–6.26 (bs, 3H, NH). ¹³C NMR (200 MHz, CDCl_3) δ 159.22 (CON), 150.07 (CH), 141.09 (Ph-C-N), 138.67 (C4), 138.05 (C2), 130.06 (C6), 129.4 (C1), 128.7 (C5), 128.47 (C-CON), 94.05 (C3). MS (CI+) m/z : 312.968; 313.979; 314.99 (MH⁺, 40; 100; 20). HRMS: calcd for $\text{C}_{10}\text{H}_9\text{N}_3\text{OI}$ (MH⁺, CI+) 313.979 found 313.9793.

4-(3-Chlorophenyl)-1H-imidazole-5-carboxamide (8b). Compound **8b** was obtained as a white solid in 20% yield; mp 160 °C. ¹H NMR (600 MHz, acetone- d_6) δ 8.54 (t, 1H, $J = 1.8$; 0.6 Hz, $H\text{-C}2$), 8.36–8.34 (dt, 1H, $J = 7.8$; 1.8 Hz, $H\text{-C}4$), 8.34 (s, 1H, CH), 7.47–7.46 (t, 1H, $J = 7.8$ Hz, $H\text{-C}5$), 7.44–7.42 (ddd, 1H, $J = 7.8$; 1.8; 1.2 Hz, $H\text{-C}6$). ¹³C NMR (300 MHz, CDCl_3) δ 158.88 (CON), 149.87 (CH), 142.64 (Ph-C-N), 138.82 (C1), 134.29 (C3), 131.45 (C-CON), 129.76 (C5), 129.57 (C4), 129.25 (C2), 127.51 (C6). MS (CI+) m/z : 222.04; 223.04; 224.04 (MH⁺, 100; 56; 37). HRMS: calcd for $\text{C}_{10}\text{H}_9\text{N}_3\text{OCl}$ (MH⁺, CI+) 222.0434 found 222.0403.

4-(3-Bromo-4-chlorophenyl)-1H-imidazole-5-carboxamide (8c). Compound **8c** was obtained as a white solid in 5% yield from compound **7c**. ¹H NMR (300 MHz, acetone- d_6) δ 8.91–8.9 (d, 1H, $J = 2.1$ Hz, $H\text{-C}2$), 8.47–8.43 (dd, 1H, $J = 8.7$; 2.1 Hz, $H\text{-C}6$), 8.38 (s, 1H, CH), 7.67–7.65 (d, 1H, $J = 8.7$ Hz, $H\text{-C}5$), 7.58 (bs, 1H, NH), 7.15 (bs, 1H, NH). ¹³C NMR (300 MHz, acetone- d_6) δ 159.5 (CON), 151.82 (CH), 141.5 (Ph-C-N), 137 (C4), 134.99 (C2), 131.65 (C1), 130.9 (C5), 130.53 (C-CON), 130.38 (C6), 122.26 (C3).

4-(3-Benzoylphenyl)-1H-imidazole-5-carboxamide (8d). Compound **8d** was obtained as a white solid in 7% yield from compound **7d**. ¹H NMR (600 MHz, CDCl_3) δ 8.65–8.64 (t, 1H, $J = 1.2$ Hz, $H\text{-C}2$), 8.51–8.49 (dt, 1H, $J = 7.8$; 1.2 Hz, $H\text{-C}4$), 7.94 (s, 1H, CH), 7.87–7.86 (m, 3H, $H\text{-C}6$, Ph), 7.6–7.59 (m, 2H, $H\text{-C}5$, Ph), 7.52–7.5 (m, 2H, Ph), 6.37 (bs, 1H, NH), 6.04 (bs, 1H, NH). ¹³C NMR (600 MHz, CDCl_3) δ 195.34 (CO), 159.02 (CON), 149.98 (CH), 143.06 (Ph-C-N), 137.64 ($Ph\text{-q}$), 137.29 (C3), 133.2 (Ph), 132.57 (C6), 131.07 (C2), 130.9 (C4), 130.22 (Ph), 130.02 (C5), 129.99 (C1), 129.41 (C-CONH₂), 128.32 (Ph). MS (ES+) m/z : 293 (MH⁺, 70), 315 (MNa⁺, 100). HRMS: calcd for $\text{C}_{17}\text{H}_{14}\text{N}_3\text{O}_2$ (MH⁺, CI+) 292.1086 found 292.1078.

4-(3-Phenylphenyl)-1H-imidazole-5-carboxamide (8e). Compound **8e** was obtained from **7e** by general procedure 5. The crude mixture was purified by column chromatography (eluent hexane/EtOAc = 1:1) to give the desired compound as a yellow solid in 15.3% yield. ¹H NMR (200 MHz, CDCl_3) δ 8.52–8.5 (td, 1H, $J = 1.93$; 0.64 Hz, $H\text{-C}2$), 8.21–8.16 (ddd, 1H, $J = 7.5$; 1.93; 1.12 Hz, $H\text{-C}4$), 7.94 (s, 1H, CH), 7.7–7.3 (m, 7H, $H\text{-C}5$, $H\text{-C}6$, Ph), 6.34–6 (bs, 3H, NH , NH_2). ¹³C NMR (300 MHz, CDCl_3 , ppm δ): 159.44 (CON), 150.13 (CH), 141.32 (Ph-C-N), 140.86 (Ph), 130.82 (C1), 130.33 (C3), 129.22 (C-CONH₂), 128.94 (Ph), 128.53 (C5), 128.31 (C4), 128.24 (C6), 127.57 (C2), 127.34 (Ph).

4-Phenyl-1H-imidazole-5-carboxamide (8g). Compound **8g** was obtained as a yellow solid in 80% yield from compound **7g**. ¹H NMR (300 MHz, CDCl_3) δ 8.19–8.15 (m, 2H, $H\text{-C}2$), 7.91 (s, 1H, CH), 7.46–7.37 (m, 3H, $H\text{-C}3$, $H\text{-C}4$), 6.49–6.36 (bs, 1H,

NH), 6.36–6.29 (bs, 1H, *NH*). ¹³C NMR (200 MHz, CDCl₃) δ 159.5 (*CON*), 149.96 (*CH*), 143.68 (Ph-C-N), 131.9 (C1), 129.6 (C3), 129.21 (C4), 128.24 (C2), 124.87 (C-CONH₂). MS (ES+) *m/z*: 171 ([M - NH₂], 40), 189 (MDH⁺, 100), 211 (MDNa⁺, 40).

General Procedure for the Synthesis of Amino-thiazoles 9a–g.⁵³ Thiourea (0.265 mmol) was dissolved in 95% EtOH (10 mL) followed by addition of an α-bromoketone (0.265 mmol). The reaction mixture was stirred at room temperature and evaluated with TLC (hexane/EtOAc = 2:1). The reaction was stopped after 4 h when no starting material spot was detected. Evaporation of the reaction mixture to dryness and recrystallization from MeOH/Et₂O provided the desired product.

2-Amino-4-(3-iodophenyl)thiazole-5-carboxamide Hydrobromide (9a). Compound **9a** was obtained as a yellow solid in 72% yield from **7a**; mp 248–250 °C. ¹H NMR (200 MHz, CD₃OD) δ 8.03–8.01 (td, 1H, *J* = 1.68; 0.38 Hz, *H-C2*), 7.99–7.93 (ddd, 1H, *J* = 7.9; 1.68; 1 Hz, *H-C6*), 7.67–7.62 (ddd, 1H, *J* = 7.9; 1.68; 1 Hz, *H-C4*), 7.37–7.3 (td, 1H, *J* = 7.9; 0.38 Hz, *H-C5*). ¹³C NMR (300 MHz, CD₃OD) δ 170.79 (C-NH₂), 162.95 (*CON*), 141.37 (C4), 140.18 (Ph-C-N), 139.1 (C2), 131.95 (C6), 130.69 (C1), 129.85 (C5), 117.54 (C-CONH₂), 95.18 (C3). MS (CI+) *m/z*: 345.951 (MH⁺, 35). HRMS: calcd for C₁₀H₉N₃O₂S (MH⁺, CI+) 345.9511 found 345.9508.

2-Amino-4-(3-chlorophenyl)thiazole-5-carboxamide Hydrobromide (9b). Compound **9b** was obtained as a yellow solid in 72% yield from **7b**; mp 138–140 °C. ¹H NMR (300 MHz, CD₃OD) δ 7.71–7.7 (m, 1H, *H-C2*), 7.66–7.56 (m, 3H, *H-C4*, *H-C5*, *H-C6*). ¹³C NMR (200 MHz, CD₃OD) δ 170.6 (C-NH₂), 162.83 (*CON*), 140.09 (Ph-C-N), 136.17 (C3), 136.14 (C1), 132.41 (C5), 131.96 (C4), 130.44 (C2), 121.99 (C6), 117.77 (C-CONH₂).

2-Amino-4-(3-bromo-4-chlorophenyl)thiazole-5-carboxamide Hydrobromide (9c). Compound **9c** was obtained as a white solid in 72% yield from **7c**; mp 245–247 °C. ¹H NMR (300 MHz, CD₃OD) δ 8 (d, 1H, *J* = 2.1 Hz, *H-C2*), 7.73–7.7 (d, 1H, *J* = 8.4 Hz, *H-C5*), 7.65–7.59 (dd, 1H, *J* = 8.4; 2.1 Hz, *H-C6*). ¹³C NMR (200 MHz, CD₃OD) δ 170.73 (C-NH₂), 162.83 (*CON*), 139.47 (Ph-C-N), 138.38 (C4), 135.75 (C2), 132.11 (C5), 131.03 (C6), 130.6 (C1), 129.02 (C3), 122.81 (C-CONH₂). MS (CI+) *m/z*: 332.915 (M⁺, 100). HRMS: calcd for C₁₀H₇N₃O₂SClBr (M⁺, CI+) 332.9161 found 332.9153.

2-Amino-4-(3-benzoylphenyl)thiazole-5-carboxamide Hydrobromide (9d). Compound **9d** was obtained as a highly hygroscopic, yellow solid in 72% yield from **7d**. ¹H NMR (300 MHz, acetone-*d*₆) δ 8.06–8.05 (t, 1H, *J* = 1.8 Hz, *H-C2*), 7.99–7.96 (ddd, 1H, *J* = 7.8; 1.8; 1.5 Hz, *H-C6*), 7.87–7.8 (m, 3H, *H-C4*, *H-C5*, *Ph*), 7.7–7.55 (m, 4H, *Ph*). ¹³C NMR (300 MHz, CD₃OD) δ 196.98 (*CO*), 170.86 (C-NH₂), 162.99 (*CON*), 141.26 (Ph-C-N), 139.67 (*Ph*), 138.09 (C3), 134.27 (*Ph*), 133.35 (C6), 131.85 (C2), 131.15 (*Ph*), 130.58 (C4), 130.47 (C1), 129.75 (*Ph*, C5), 129.26 (C-CONH₂). MS (CI+) *m/z*: 324.076 (MH⁺, 100). HRMS: calcd for C₁₇H₁₄N₃O₂S (MH⁺, CI+) 324.0807 found 324.0759.

2-Amino-4-(3-phenylphenyl)thiazole-5-carboxamide Hydrobromide (9e). Compound **9e** was obtained as a yellow solid in 55% yield from **7e**; mp 223–227 °C. ¹H NMR (300 MHz, CD₃OD) δ 7.9–7.85 (m, 2H, *H-C2*, *H-C4*), 7.74–7.59 (m, 4H, *H-C5*, *H-C6*, *Ph*), 7.5–7.45 (m, 2H, *Ph*), 7.39–7.36 (m, 1H, *Ph*). ¹³C NMR (300 MHz, CD₃OD) δ 170.75 (C-NH₂), 163.15 (*CON*), 143.59 (Ph-C-N), 141.41 (*Ph*), 140.83 (C1), 132.58 (C3), 131.07 (C5), 130.95 (C4), 130.13 (*Ph*), 129.83 (C-CONH₂), 129.17 (C6), 129.14 (*Ph*), 128.96 (C2), 128.12 (*Ph*). MS (CI+) *m/z*: 295.078 (M⁺, 10). HRMS: calcd for C₁₆H₁₃N₃O₂S (M⁺, CI+) 295.0779 found 295.0779.

2-Amino-4-phenylthiazole-5-carboxamide Hydrobromide (9g).⁵⁴ Compound **9g** was obtained as a yellow solid in 59% yield from **7g**; mp 225–230 °C. ¹H NMR (200 MHz, DMSO-*d*₆) δ 7.59–7.56 (m, 2H, *H-C2*), 7.52–7.49 (m, 3H, *H-C3*, *H-C4*), 7.17–7.0 (bs, 1H, *NH*), 5.27–5.11 (bs, 3H, *NH*). ¹³C NMR (200 MHz, DMSO-*d*₆) δ 167.92 (C-NH₂), 161.2 (*CON*), 143.25 (Ph-C-N), 129.94 (C1), 129.85 (C4), 129.17 (C3), 128.48 (C2), 114.9 (C-CONH₂). MS (CI+) *m/z*: 219.045 (M⁺, 100). HRMS: calcd for C₁₀H₉N₃O₂S (M⁺, CI+) 219.0433 found 219.0452.

General Procedure for the Synthesis of Thiazoles 10a–g.⁵⁵ To an aminothiazole derivative **9a–g** (0.5 mmol) dissolved in 40% H₂SO₄ (6 mL) at 0 °C was added NaNO₂ (0.9 mmol) in H₂O (0.3 mL), and the resulting yellow mixture was stirred at this temperature for 30 min. The mixture was then added to a suspension of Ca-(H₂PO₄)₂ (0.5 mmol) in water (2.15 mL), and the final mixture was stirred at 0 °C for additional 1 h. The obtained suspension was filtered, the residue washed with CHCl₃, and the filtrate further extracted with CHCl₃. The organic phase washed with brine, dried over MgSO₄, and evaporated. The crude residue was purified by column chromatography (eluent hexane/EtOAc = 2:1) to provide compounds **10a–g**.

4-(3-Iodophenyl)thiazole-5-carboxamide (10a). Compound **10a** was obtained from **9a** as a yellow solid in 15.8% yield; mp 137–140 °C. ¹H NMR (300 MHz, CDCl₃) δ 8.9 (s, 1H, *CH*), 8.06–8.05 (t, 1H, *J* = 1.5 Hz, *H-C2*), 7.84–7.8 (ddd, 1H, *J* = 7.8; 1.5 Hz, *H-C4*), 7.67–7.63 (ddd, 1H, *J* = 7.8; 1.5 Hz, *H-C6*), 7.26–7.2 (t, 1H, *J* = 7.8 Hz, *H-C5*), 5.99–5.77 (bs, 2H, *NH*). ¹³C NMR (300 MHz, CDCl₃) δ 163.26 (*CON*), 155.35 (*CH*), 139.2 (C1), 138.8 (C4), 138.23 (C2), 135.42 (Ph-C-N), 130.66 (C5), 129.36 (C-CONH₂), 128.62 (C6), 94.83 (C3). C₁₀H₇N₂O₂S (M⁺, CI+) 329.9324 found 329.9315.

4-(3-Chlorophenyl)thiazole-5-carboxamide (10b). Compound **10b** was obtained from **9b** as a yellow solid in 12% yield; mp 183–185 °C. ¹H NMR (300 MHz, CD₃OD) δ 9.1 (s, 1H, *CH*), 7.84–7.82 (m, 1H, *H-C2*), 7.75–7.72 (ddd, 1H, *J* = 6.3; 2.7; 1.8 Hz, *H-C4*), 7.47–7.43 (m, 2H, *H-C5*, *H-C6*). ¹³C NMR (300 MHz, CD₃OD) δ 165.26 (*CON*), 155.13 (*CH*), 153.9 (Ph-C-N), 136.84 (C3), 134.98 (C1), 130.92 (C5), 129.85 (C4), 129.73 (C2), 129.53 (C-CONH₂), 128.36 (C6). MS (CI+) *m/z*: 237.997; 238.986; 239.996 (M⁺, 90; 60; 36). HRMS: calcd for C₁₀H₇N₂O₂SCl (M⁺, CI+) 237.9968 found 237.9968.

4-(3-Bromo-4-chlorophenyl)thiazole-5-carboxamide (10c). Compound **10c** was obtained from **9c** as a white solid in 13% yield; mp 154–156 °C. ¹H NMR (300 MHz, acetone-*d*₆) δ 9.09 (s, 1H, *CH*), 8.2–8.19 (d, 1H, *J* = 2.1 Hz, *H-C2*), 7.87–7.84 (dd, 1H, *J* = 8.4; 2.1 Hz, *H-C6*), 7.66–7.63 (d, 1H, *J* = 8.4 Hz, *H-C5*), 7.35 (bs, 1H, *NH*), 7.16 (bs, 1H, *NH*). ¹³C NMR (300 MHz, acetone-*d*₆) δ 163.64 (*CON*), 154.57 (*CH*), 135.64 (Ph-C-N), 134.99 (C2), 134.82 (C4), 131.6 (C1), 131.1 (C5), 130.46 (C6), 129.25 (C3), 122.41 (C-CONH₂). MS (CI+) *m/z*: 316.903 (M⁺, 100), 317.904 (MH⁺, 90). HRMS: calcd for C₁₀H₆N₃O₂SCl³⁵Br (MH⁺, CI+) 298.9461 found 298.9438.

4-(3-Benzoylphenyl)thiazole-5-carboxamide (10d). Compound **10d** was obtained from **9d** as a yellow solid in 12% yield; mp 180–183 °C. ¹H NMR (300 MHz, CDCl₃) δ 8.91 (s, 1H, *CH*), 8.11–8.1 (t, 1H, *J* = 1.8 Hz, *H-C2*), 7.94–7.89 (m, 2H, *H-C4*, *H-C6*), 7.83–7.8 (m, 2H, *Ph*), 7.65–7.58 (m, 2H, *H-C5*, *Ph*), 7.52–7.46 (m, 2H, *Ph*), 5.84–5.82 (bs, 2H, *NH*). ¹³C NMR (300 MHz, CDCl₃) δ 195.87 (*CO*), 162.54 (*CON*), 155.07 (*CH*), 154.32 (Ph-C-N), 138.46 (*Ph*), 136.92 (C3), 133.73 (C1), 133.12 (C6), 132.87 (C2), 131.04 (C4), 130.82 (C5), 130.08 (Ph), 129.08 (*Ph*), 128.49 (C-CONH₂), 128.48 (*Ph*). MS (CI+) *m/z*: 231.004 ([M - Ph], 60), 308.063 (M⁺, 100). HRMS: calcd for C₁₇H₁₂N₂O₂S (M⁺, CI+) 308.0619 found 308.0634.

4-(3-Phenylphenyl)thiazole-5-carboxamide (10e). Compound **10e** was obtained from **9e** as a yellow solid in 12% yield. ¹H NMR (300 MHz, CDCl₃) δ 8.92 (s, 1H, *CH*), 7.91–7.89 (td, 1H, *J* = 1.8; 0.6 Hz, *H-C2*), 7.74–7.71 (dt, 1H, *J* = 7.5; 1.5 Hz, *H-C4*), 7.64–7.55 (m, 4H, *H-C5*, *H-C6*, *Ph*), 7.5–7.35 (m, 3H, *Ph*), 5.79–5.72 (bs, 2H, *NH*). ¹³C NMR (300 MHz, CDCl₃) δ 164.25 (*CON*), 155.33 (*CH*), 129.64 (C5), 128.98 (*Ph*), 128.54 (C4), 128.23 (*Ph*), 128.17 (C6), 127.92 (C2), 127.19 (*Ph*). MS (CI+) *m/z*: 264.094 ([M - NH₂]⁺, 40), 280.071 (M⁺, 100). HRMS: calcd for C₁₆H₁₂N₂O₂S (M⁺, CI+) 280.067 found 280.0713.

4-Phenylthiazole-5-carboxamide (10g). Compound **10g** was obtained from **9g** as a yellow solid in 16% yield; mp 150 °C. ¹H NMR (300 MHz, CDCl₃) δ 8.91 (s, 1H, *CH*), 7.66–7.63 (m, 2H, *H-C2*), 7.54–7.49 (m, 2H, *H-C3*, *H-C4*), 6.46 (bs, 1H, *NH*), 5.8 (bs, 1H, *NH*). ¹³C NMR (300 MHz, CDCl₃) δ 163.42 (*CON*), 155.49 (*CH*, Ph-C-N), 133.57 (C1), 130.01 (C3), 129.75 (C-CONH₂),

129.51 (C4), 129.31 (C2). MS (CI+) m/z : 204.038 (M⁺, 100), 205.045 (MH⁺, 90). HRMS: calcd for C₁₀H₉N₂O₅ (MH⁺, CI+) 205.0436 found 205.0453.

Biology. Expression and Purification of RTs. Wild-type p66/p51 HIV-1 RT, derived from BH-10 clone of HIV-1, was expressed in bacteria. This enzyme, which has six histidines tag at the C-terminus of the p66 subunit, was purified on Ni²⁺ nitrilotriacetic acid agarose (Ni-NTA) column followed by cation exchange chromatography, as was previously described.⁵⁶ The plasmids encoding for the single mutant T181C and double mutant L100I + K103N were a kind gift from Dr. S. Hughes of NCI, NIH in Frederick, MD. The mutant T181C RT was expressed and purified in a similar manner on Ni-NTA column. The double mutant L100I-K103N was expressed as a homodimer enzyme with two identical 66 kDa subunits; it was expressed in DH5 α *E. coli* and purified in a similar manner as above.

DNA Polymerase Assay. The DNA polymerase activity of RT was assayed by measuring the incorporation of [³H]dTTP into poly(rA)_n·oligo(dT)_{12–18} template-primer as described previously.⁵⁷ All inhibitors were serially diluted (5-fold or 3-fold for assays with compounds **8c** and **5f**) in DMSO, and 1 μ L of each concentration (or 1 μ L of DMSO only as a control) was added to 79 μ L of 31.25 mM Tris-HCl pH 7.5, 50 mM KCl, and 8 mM MgCl₂. A 10 μ L amount of purified HIV-1 RT (14 ng) was added to each tube, and the solutions were incubated on ice for 10 min. The enzymatic reactions were initiated by the addition of 10 μ L of the substrate mix [50 μ g/mL poly(rA)_n·oligo(dT)_{12–18}, 50 μ M dTTP, 150 μ Ci/mL [³H]dTTP] followed by incubation for 30 min at 37 °C. The reaction was stopped by adding 50 μ g/mL herring sperm carrier DNA and 40 mM sodium pyrophosphate followed by precipitation with ice-cold 10% (w/v) trichloroacetic acid. The precipitates were collected on Whatman GF/C fiberglass filters, and the filters were washed with 5% cold trichloroacetic acid and then with 50% cold ethanol. The dried filters were put in a scintillation fluid and counted in a β scintillation counter.

The reported measurements are the average of at least two experiments for compounds with IC₅₀ values higher than 10 μ M and at least three experiments for compounds with IC₅₀ values lower than 10 μ M. The dose–response curves were nonlinearly fitted to the four-parameter logistic equation⁵⁸ using Origin software.

RNase H Assay. The RNase H activity of RT was assayed with fluorescence resonance energy transfer technology as described previously.⁵⁹ Briefly, RT was incubated with a substrate of hybrid of fluorescein–RNA and DNA–4-[[4'-(dimethylamino)phenyl]azo]-benzoic acid and with (or without) a specific inhibitor. Hydrolysis of the substrate and the resulting emitting fluorescence was measured with a fluorescence spectrometer after 30 min of incubation at 37 °C. To improve the signal-to-noise ratio, the assay was slightly modified to contain 6 nM RT and 1 mM DTT. All measurements were done in triplicates in a 96-well plate, and IC₅₀ values were interpolated from the dose–response curves.

PAGE Mobility Shift Assay. Complex formation between [³²P]-5' end labeled DNA oligonucleotide and HIV-1 RT was detected by the electrophoretic retardation of the DNA as a result of its association with RT, as previously described in detail.⁶⁰ HIV-1 RT (1.5 pmol) was preincubated with or without compounds **8c**, **5f**, and nevirapine, each at a final concentration of 250 and 625 μ M, in addition to 50 μ M toxiusol that served as a positive control.²³ After 10 min at 4 °C, the binding reactions were initiated by the addition of 0.12 pmol of the [³²P]-end labeled double-stranded DNA substrate. This substrate was a duplex of two 54 nt-long synthetic oligonucleotide. The first one with the sequence:

5'-AATGAAAGACCCACCTGTAGGTTGGATCCTTAC-CCGTCAGCGGGGCTTTCA-3' was 5'-end labeled and the second one with the sequence:

5'-AATGAAAGACCCCGCTGACGGGTAAGGATCCAAC-CTACAGGTGGGGTCTTTCA-3'. After annealing, the resulting double-stranded DNA had two base overhangs on both 5' ends. The binding reaction assays were conducted in a final volume of 12.5 μ L, containing 10 mM HEPES, 30 mM ammonium sulfate, 0.25 mM dithiothreitol, 0.1 mg/mL bovine serum albumin, and 10

mM KCl, at final pH 8.0. These reactions were further incubated for 10 min at 32 °C and were stopped by the addition of 2 μ L of loading buffer (1% bromophenol blue, 30% glycerol). The reaction mixtures underwent electrophoresis through 6.5% polyacrylamide nondenatured gel in TBE buffer (89 mM Tris base, 89 mM borate, and 2 mM EDTA, pH 8.3) at 4 °C under 15 V/cm for about 2.5 h. The dried gels were subjected to autoradiography at –80 °C.

DNA-Primer Extension Reactions. Single-stranded circular ϕ X174am3 DNA that served as a template was primed with a synthetic 15-mer oligonucleotide (5'-AAAGCGAGGGTATCC-3'), which hybridizes at positions 588–602 of the template-DNA.²² The primer, prelabeled at its 5'-end with [γ -³²P] ATP using T4 polynucleotide kinase, was annealed to a 2-fold molar excess of unlabeled template DNA. The reactions were performed in 6.6 mM Tris-HCl, pH 8.0, 4 mM DTT, 6 mM MgCl₂, 24 μ g/mL bovine serum albumin, 33 mM NaCl, 4 nM template-primer, and all four dNTPs (each at a final concentration of 20 μ M) and 1.6 nM of purified HIV-1 RT. The reactions, each at a final volume of 12.5 μ L, were incubated at 37 °C for 30 min and were stopped by adding 12.5 μ L of formamide loading buffer (90% formamide, 10 mM EDTA, 1 mg/mL bromophenol blue, 1 mg/mL xylene cyanole). The samples were heat-denatured, quickly cooled on ice, and loaded onto 6 M urea 12% polyacrylamide denaturing gels, followed by electrophoresis (urea-PAGE) as previously described.²² The gels were dried and subjected to autoradiography at –80 °C or at room temperature to obtain a close to linear exposure.

Cytotoxic Assay. Cytotoxic assay was performed in 96-well plate with XTT substrate as previously described.⁶¹ Absorbance was recorded at 450 nm and the reference wavelength was recorded at 620 nm.

Acknowledgment. The authors thank Dr. S. Loya and Dr. R. Shultz for helpful comments on the manuscript, Dr. S. H. Hughes from NCI for sending us the plasmids that express the mutant HIV-1 RTs studied here, and to Dr. M. A. Parniak from University of Pittsburgh, School of Medicine, for the substrate for the RNase H assay. We also thank Dr. A. N. Jain for kindly supplying the sufex software, Accelrys inc. for access to Cerius 2 software and Dr. H. Senderowitz for constructive guidance to the molecular modeling studies. The generous support for this work by the “Marcus Center for Pharmaceutical and Medicinal Chemistry” at Bar Ilan University is gratefully acknowledged.

References

- Coffin, J. M.; Hughes, S. H.; Varmus, H. E. *Retroviruses*; Cold Spring Harbor Laboratory Press: Woodbury, NY, 1997.
- De Clercq, E. Antiviral drugs in current clinical use. *J. Clin. Virol.* **2004**, *30*, 115–133.
- Das, K.; Lewi, P. J.; Hughes, S. H.; Arnold, E. Crystallography and the design of anti-AIDS drugs: conformational flexibility and positional adaptability are important in the design of non-nucleoside HIV-1 reverse transcriptase inhibitors. *Prog. Biophys. Mol. Biol.* **2005**, *88*, 209–231.
- Ren, J.; Diprose, J.; Warren, J.; Esnouf, R. M.; Bird, L. E.; Ikemizu, S.; Slater, M.; Milton, J.; Balzarini, J.; Stuart, D. I.; Stammers, D. K. Phenylethylthiazolylthiourea (PETT) non-nucleoside inhibitors of HIV-1 and HIV-2 reverse transcriptases. Structural and biochemical analyses. *J. Biol. Chem.* **2000**, *275*, 5633–5639.
- De Clercq, E. HIV-chemotherapy and -prophylaxis: new drugs, leads and approaches. *Int. J. Biochem. Cell Biol.* **2004**, *36*, 1800–1822.
- Sarafianos, S. G.; Das, K.; Hughes, S. H.; Arnold, E. Taking aim at a moving target: designing drugs to inhibit drug-resistant HIV-1 reverse transcriptases. *Curr. Opin. Struct. Biol.* **2004**, *14*, 716–730.
- Clavel, F.; Hance, A. J. HIV drug resistance. *N. Engl. J. Med.* **2004**, *350*, 1023–1035.
- Das, K.; Clark, A. D., Jr.; Lewi, P. J.; Heeres, J.; De Jonge, M. R.; Koymans, L. M.; Vinkers, H. M.; Daeyaert, F.; Ludovici, D. W.; Kukla, M. J.; De Corte, B.; Kavash, R. W.; Ho, C. Y.; Ye, H.; Lichtenstein, M. A.; Andries, K.; Pauwels, R.; De Bethune, M. P.; Boyer, P. L.; Clark, P.; Hughes, S. H.; Janssen, P. A.; Arnold, E. Roles of conformational and positional adaptability in structure-based

- design of TMC125-R165335 (etravirine) and related non-nucleoside reverse transcriptase inhibitors that are highly potent and effective against wild-type and drug-resistant HIV-1 variants. *J. Med. Chem.* **2004**, *47*, 2550–2560.
- (9) Masuda, N.; Yamamoto, O.; Fujii, M.; Ohgami, T.; Fujiyasu, J.; Kontani, T.; Moritomo, A.; Orita, M.; Kurihara, H.; Koga, H.; Kageyama, S.; Ohta, M.; Inoue, H.; Hatta, T.; Shintani, M.; Suzuki, H.; Sudo, K.; Shimizu, Y.; Kodama, E.; Matsuoka, M.; Fujiwara, M.; Yokota, T.; Shigeta, S.; Baba, M. Studies of non-nucleoside HIV-1 reverse transcriptase inhibitors. Part 2: synthesis and structure-activity relationships of 2-cyano and 2-hydroxy thiazolidenebenzenesulfonamide derivatives. *Bioorg. Med. Chem.* **2005**, *13*, 949–961.
- (10) Romines, K. R.; Freeman, G. A.; Schaller, L. T.; Cowan, J. R.; Gonzales, S. S.; Tidwell, J. H.; Andrews, C. W., 3rd; Stammers, D. K.; Hazen, R. J.; Ferris, R. G.; Short, S. A.; Chan, J. H.; Boone, L. R. Structure-activity relationship studies of novel benzophenones leading to the discovery of a potent, next generation HIV nonnucleoside reverse transcriptase inhibitor. *J. Med. Chem.* **2006**, *49*, 727–739.
- (11) Shoichet, B. K. Virtual screening of chemical libraries. *Nature* **2004**, *432*, 862–865.
- (12) Schneider, G.; Fechner, U. Computer-based de novo design of drug-like molecules. *Nat. Rev. Drug Discovery* **2005**, *4*, 649–663.
- (13) Mao, C.; Sudbeck, E. A.; Venkatchalam, T. K.; Uckun, F. M. Structure-based drug design of non-nucleoside inhibitors for wild-type and drug-resistant HIV reverse transcriptase. *Biochem. Pharmacol.* **2000**, *60*, 1251–1265.
- (14) Vinkers, H. M.; de Jonge, M. R.; Daeyaert, F. F.; Heeres, J.; Koymans, L. M.; van Lenthe, J. H.; Lewi, P. J.; Timmerman, H.; Van, Aken, K.; Janssen, P. A. SYNOPSIS: SYNthesize and OPTimize System in Silico. *J. Med. Chem.* **2003**, *46*, 2765–2773.
- (15) Corbett, J. W.; Ko, S. S.; Rodgers, J. D.; Jeffrey, S.; Bacheler, L. T.; Klabe, R. M.; Diamond, S.; Lai, C. M.; Rabel, S. R.; Saye, J. A.; Adams, S. P.; Trainor, G. L.; Anderson, P. S.; Erickson-Viitanen, S. K. Expanded-spectrum nonnucleoside reverse transcriptase inhibitors inhibit clinically relevant mutant variants of human immunodeficiency virus type 1. *Antimicrob. Agents Chemother.* **1999**, *43*, 2893–2897.
- (16) Ren, J.; Nichols, C.; Bird, L.; Chamberlain, P.; Weaver, K.; Short, S.; Stuart, D. I.; Stammers, D. K. Structural mechanisms of drug resistance for mutations at codons 181 and 188 in HIV-1 reverse transcriptase and the improved resilience of second generation non-nucleoside inhibitors. *J. Mol. Biol.* **2001**, *312*, 795–805.
- (17) *Cerius2 LUDI user guide*; San Diego, CA, 2003.
- (18) Bohm, H. J. The computer program LUDI: a new method for the de novo design of enzyme inhibitors. *J. Comput.-Aided Mol. Des.* **1992**, *6*, 61–78.
- (19) Bohm, H. J. A novel computational tool for automated structure-based drug design. *J. Mol. Recognit.* **1993**, *6*, 131–137.
- (20) Venkatchalam, C. M.; Jiang, X.; Oldfield, T.; Waldman, M. LigandFit: a novel method for the shape-directed rapid docking of ligands to protein active sites. *J. Mol. Graph. Model* **2003**, *21*, 289–307.
- (21) Kortekaas, T. A.; Cerfontain, H. Aromatic sulfonation. Part 66. Sulfonation of some biphenyl derivatives. *J. Chem. Soc., Perkin Trans. 2* **1979**, *2*, 224–227.
- (22) Avidan, O.; Meer, M. E.; Oz, I.; Hizi, A. The processivity and fidelity of DNA synthesis exhibited by the reverse transcriptase of bovine leukemia virus. *Eur. J. Biochem.* **2002**, *269*, 859–867.
- (23) Loya, S.; Bakhanashvili, M.; Kashman, Y.; Hizi, A. Mechanism of inhibition of HIV reverse transcriptase by toxiusol, a novel general inhibitor of retroviral and cellular DNA polymerases. *Biochemistry* **1995**, *34*, 2260–2266.
- (24) Erlanson, D. A.; McDowell, R. S.; O'Brien, T. Fragment-based drug discovery. *J. Med. Chem.* **2004**, *47*, 3463–3482.
- (25) Maly, D. J.; Choong, I. C.; Ellman, J. A. Combinatorial target-guided ligand assembly: identification of potent subtype-selective c-Src inhibitors. *Proc. Natl. Acad. Sci. U.S.A.* **2000**, *97*, 2419–2424.
- (26) Pellicchia, M.; Sem, D. S.; Wuthrich, K. NMR in drug discovery. *Nat. Rev. Drug Discovery* **2002**, *1*, 211–219.
- (27) Tsao, D. H.; Sutherland, A. G.; Jennings, L. D.; Li, Y.; Rush, T. S., III; Alvarez, J. C.; Ding, W.; Dushin, E. G.; Dushin, R. G.; Haney, S. A.; Kenny, C. H.; Malakian, A. K.; Nilakantan, R.; Mosyak, L. Discovery of novel inhibitors of the ZipA/FtsZ complex by NMR fragment screening coupled with structure-based design. *Bioorg. Med. Chem.* **2006**, *14*, 7953–7961.
- (28) Hizi, A.; Hughes, S. H.; Shaharabany, M. Mutational analysis of the ribonuclease H activity of human immunodeficiency virus 1 reverse transcriptase. *Virology* **1990**, *175*, 575–580.
- (29) Veber, D. F.; Johnson, S. R.; Cheng, H. Y.; Smith, B. R.; Ward, K. W.; Kopple, K. D. Molecular properties that influence the oral bioavailability of drug candidates. *J. Med. Chem.* **2002**, *45*, 2615–2623.
- (30) Lipinski, C. A.; Lombardo, F.; Dominy, B. W.; Feeney, P. J. Experimental and computational approaches to estimate solubility and permeability in drug discovery and development settings. *Adv. Drug. Delivery Rev.* **2001**, *46*, 3–26.
- (31) Bohm, H. J. Prediction of binding constants of protein ligands: a fast method for the prioritization of hits obtained from de novo design or 3D database search programs. *J. Comput.-Aided Mol. Des.* **1998**, *12*, 309–323.
- (32) Jain, A. N. Surfex: fully automatic flexible molecular docking using a molecular similarity-based search engine. *J. Med. Chem.* **2003**, *46*, 499–511.
- (33) Jones, S.; Seltsianos, D. A simple and effective method for phosphoryl transfer using TiCl₄ catalysis. *Org. Lett.* **2002**, *4*, 3671–3673.
- (34) Bumagin, N. A.; Bykov, V. V. Ligandless palladium catalyzed reactions of arylboronic acids and sodium tetraphenylborate with aryl halides in aqueous media. *Tetrahedron* **1997**, *53*, 14437–14450.
- (35) McElvain, S. M.; Carney, T. P. Piperidine derivatives. XVII. Local anesthetics derived from substituted piperidino alcohols. *J. Am. Chem. Soc.* **1946**, *68*, 2592–2600.
- (36) Beak, P.; Musick, T. J.; Chen, C. W. Does formal intramolecular transfer of an acidic deuteron to a site of halogen-lithium exchange show that lithium-halogen exchange is faster than loss of the acidic deuteron? Evidence in favor of an alternative mechanism. *J. Am. Chem. Soc.* **1988**, *110*, 3538–3542.
- (37) Rondestvedt, C. S., Jr. New syntheses of aromatic acid chlorides from trichloromethylarenes. 1. Reaction with sulfur dioxide. *J. Org. Chem.* **1976**, *41*, 3569–3574.
- (38) Pagani, G.; Baruffini, A.; Mazza, M.; Vicarini, L.; Caccialanza, G. Selective phytotoxicity of halogenated benzoic acid N,N-di-sec-butyl. *Farmaco, Ed. Sci.* **1973**, *28*, 570–589.
- (39) Ito, Y.; Kawatsuki, N.; Giri, B. P.; Yoshida, M.; Matsuura, T. Photochemistry of meta-substituted and para-substituted aromatic polycarbonyl compounds. *J. Org. Chem.* **1985**, *50*, 2893–2904.
- (40) Egle, I.; Barriault, N.; Bordeleau, M.; Drage, J.; Dube, L.; Peragine, J.; Mazzocco, L.; Arora, J.; Jarvie, K.; Tehim, A. N-(1-Benzylpyrrolidin-3-yl)arylbenzamidates as potent and selective human dopamine D4 antagonists. *Bioorg. Med. Chem. Lett.* **2004**, *14*, 4847–4850.
- (41) Yoo, S. H. Preparation of [(iodophenyl)acetoxy]choline derivatives as intermediates for chenodeoxycholic acid. US Patent 4,895,679, Jan 23, 1990.
- (42) Chen, Y.; Sieburth, S. M. A new β -keto amide synthesis. *Synthesis* **2002**, *15*, 2191–2194.
- (43) Goldstein, D. M.; Alfredson, T.; Bertrand, J.; Browner, M. F.; Clifford, K.; Dalrymple, S. A.; Dunn, J.; Freire-Moar, J.; Harris, S.; Labadie, S. S.; La Fargue, J.; Lapiere, J. M.; Larrabee, S.; Li, F.; Papp, E.; McWeeney, D.; Ramesha, C.; Roberts, R.; Rotstein, D.; San, Pablo, B.; Sjogren, E. B.; So, O. Y.; Talamas, F. X.; Tao, W.; Trejo, A.; Villasenor, A.; Welch, M.; Welch, T.; Weller, P.; Whiteley, P. E.; Young, K.; Zipfel, S. Discovery of S-[5-amino-1-(4-fluorophenyl)-1H-pyrazol-4-yl]-[3-(2,3-dihydroxypropoxy)phenyl]methanone (RO3201195), an orally bioavailable and highly selective inhibitor of p38 MAP kinase. *J. Med. Chem.* **2006**, *49*, 1562–1575.
- (44) Gao, Y.; Wang, H.; Xu, M.; Lian, H.; Pan, Y.; Shi, Y. Addition of acetonitrile anions to unsaturated systems in an ultrasonically dispersed potassium system. *Org. Prep. Proced. Int.* **2001**, *33*, 351–356.
- (45) Baraldi, P. G.; Romagnoli, R.; Pavani, M. G.; Nunez, Mdel, C.; Tabrizi, M. A.; Shryock, J. C.; Leung, E.; Moorman, A. R.; Uluoglu, C.; Iannotta, V.; Merighi, S.; Borea, P. A. Synthesis and biological effects of novel 2-amino-3-naphthoylthiophenes as allosteric enhancers of the A1 adenosine receptor. *J. Med. Chem.* **2003**, *46*, 794–809.
- (46) Collin, X.; Sauleau, A.; Coulon, J. 1,2,4-Triazolo mercapto and aminonitriles as potent antifungal agents. *Bioorg. Med. Chem. Lett.* **2003**, *13*, 2601–2605.
- (47) Gotor, V.; Liz, R.; Testera, A. M. Preparation of N-unsubstituted b-ketoamides by Rhodococcus rhodochrous-catalyzed hydration of b-ketonitriles. *Tetrahedron* **2004**, *60*, 607–618.
- (48) Campi, E. M.; Jackson, W. R.; Marcuccio, S. M.; Naeslund, C. G. M. High yields of unsymmetrical biaryls via cross coupling of arylboronic acids with haloarenes using a modified Suzuki-Beletskaya procedure. *J. Chem. Soc., Chem. Commun.* **1994**, *20*, 2395.
- (49) Kuzma, P. C.; Brown, L. E.; Harris, T. M. Generation of the dianion of N-(trimethylsilyl)acetamide and reaction of the dianion with electrophilic reagents. *J. Org. Chem.* **1984**, *49*, 2015–2018.
- (50) Suzuki, H.; Shinpo, K.; Yamazaki, T.; Niwa, S.; Yokoyama, Y.; Murakami, Y. Synthetic studies of 1,2,3,4-tetrahydro-1,3,4-trioxo-b-carboline alkaloids. *Heterocycles* **1996**, *42*, 83–86.
- (51) Pachter, I. J.; Nemeth, P. E. Pteridines. IV. Synthesis of 2,4,6-triamino-7-phenylpteridine and related compounds through the Hofmann reaction. *J. Org. Chem.* **1963**, *28*, 1203–1206.

- (52) Gao, S. Improved preparation of cimetidine intermediates. *Zhongguo Yiyao Gongye Zazhi* **1993**, *24*, 135–136.
- (53) Kurkijy, R. P.; Brown, E. V. Preparation of thiazole Grignard reagents and thiazolyl-lithium compounds. *J. Am. Chem. Soc.* **1952**, *74*, 6260–6262.
- (54) Yamaguchi, K.; Tsuji, T.; Kobori, T.; Hatanaka, Y.; Goda, K. Bone formation promoters. JP11209284, August 3, 1999.
- (55) Katsuura, K.; Mitsuhashi, K. T. Thiazole analogs of benzomorphans. III. Syntheses of 4,5,6,7,8,9-hexahydro-4,8-methano-5-methylthiazolo[4,5-c]azocine and 4,5,6,7,8,9-hexahydro-4,8-methano-5-methylthiazolo[5,4-c]azocine. *Chem. Pharm. Bull.* **1983**, *31*, 2094–2102.
- (56) Sevilya, Z.; Loya, S.; Adir, N.; Hizi, A. The ribonuclease H activity of the reverse transcriptases of human immunodeficiency viruses type 1 and type 2 is modulated by residue 294 of the small subunit. *Nucleic Acids Res.* **2003**, *31*, 1481–1487.
- (57) Hizi, A.; Tal, R.; Shaharabany, M.; Currens, M. J.; Boyd, M. R.; Hughes, S. H.; McMahon, J. B. Specific inhibition of the reverse transcriptase of human immunodeficiency virus type 1 and the chimeric enzymes of human immunodeficiency virus type 1 and type 2 by nonnucleoside inhibitors. *Antimicrob. Agents Chemother.* **1993**, *37*, 1037–1042.
- (58) DeLean, A.; Munson, P. J.; Rodbard, D. Simultaneous analysis of families of sigmoidal curves: application to bioassay, radioligand assay, and physiological dose-response curves. *Am. J. Physiol.* **1978**, *235*, E97–102.
- (59) Parniak, M. A.; Min, K. L.; Budihias, S. R.; Le Grice, S. F.; Beutler, J. A. A fluorescence-based high-throughput screening assay for inhibitors of human immunodeficiency virus-1 reverse transcriptase-associated ribonuclease H activity. *Anal. Biochem.* **2003**, *322*, 33–39.
- (60) Bakhanashvili, M.; Hizi, A. Interaction of the reverse transcriptase of human immunodeficiency virus type 1 with DNA. *Biochemistry* **1994**, *33*, 12222–12228.
- (61) Roehm, N. W.; Rodgers, G. H.; Hatfield, S. M.; Glasebrook, A. L. An improved colorimetric assay for cell proliferation and viability utilizing the tetrazolium salt XTT. *J. Immunol. Methods* **1991**, *142*, 257–265.

JM0613121